

Cholesterol- and actin-centered view of the plasma membrane: updating the Singer–Nicolson fluid mosaic model to commemorate its 50th anniversary[†]

Akihiro Kusumi^{1,2,3,*}, Taka A. Tsunoyama¹, Bo Tang¹, Koichiro M. Hirosawa¹, Nobuhiro Morone⁴, Takahiro K. Fujiwara¹, and Kenichi G. N. Suzuki^{1,2,3}

¹Membrane Cooperativity Unit, Okinawa Institute of Science and Technology Graduate University (OIST), Okinawa 904-0495, Japan; ²Institute for Integrated Cell-Material Sciences (WPI-iCeMS), Kyoto University, Kyoto 606-8501, Japan; ³Institute for Glyco-Core Research (iGCORE), Gifu University, Gifu 501-1193, Japan; ⁴MRC Toxicology Unit, University of Cambridge, Cambridge CB2 1QR, UK

ABSTRACT Two very polarized views exist for understanding the cellular plasma membrane (PM). For some, it is the simple fluid described by the original Singer–Nicolson fluid mosaic model. For others, due to the presence of thousands of molecular species that extensively interact with each other, the PM forms various clusters and domains that are constantly changing and therefore, no simple rules exist that can explain the structure and molecular dynamics of the PM. In this article, we propose that viewing the PM from its two predominant components, cholesterol and actin filaments, provides an excellent and transparent perspective of PM organization, dynamics, and mechanisms for its functions. We focus on the actin-induced membrane compartmentalization and lipid raft domains coexisting in the PM and how they interact with each other to perform PM functions. This view provides an important update of the fluid mosaic model.

Monitoring Editor

William Bement
University of Wisconsin,
Madison

Received: Dec 6, 2021

Revised: Dec 7, 2022

Accepted: Feb 7, 2023

INTRODUCTION

When we consider plasma membrane (PM) structure, dynamics, and functions, we are often struck by the feeling that we are engaged in military intelligence, facing the so-called VUCA problems: volatility, uncertainty, complexity, and ambiguity (Bennis and Nanus, 1986).

DOI:10.1091/mbc.E20-12-0809

[†]Dedicated to our mentors, Ohnishi-sensei, Jim, and Mal.

*Address correspondence to: Akihiro Kusumi (akihiro.kusumi@oist.jp).

Abbreviations used: ALO, anthrolysin O; BCR, B-cell receptor; CHOL, cholesterol; DOPC, 1- α -dioleoylphosphatidylcholine; DRM, detergent-resistant membrane; DSPC, 1- α -distearoylphosphatidylcholine; Fc ϵ RI, high-affinity Fc ϵ receptor; FRET, Förster resonance energy transfer; GPI, glycosylphosphatidylinositol; GPI-AP, GPI-anchored protein; GPMV, giant plasma membrane vesicle; GUV, giant unilamellar vesicle; IFV, influenza virus; Lo- and Ld-phases, liquid-ordered and liquid-disordered phases, respectively; OlyA, ostreolysin A; PALM/STORM, photoactivation/photo-conversion localization microscopy/stochastic optical reconstruction microscopy; PFO, perfringolysin O; PI, phosphatidylinositol; PM, plasma membrane; STALL, stimulation-induced arrest of lateral diffusion; STED, stimulated emission depletion TM, transmembrane; VUCA, volatility, uncertainty, complexity, and ambiguity.

© 2023 Kusumi et al. This article is distributed by The American Society for Cell Biology under license from the author(s). Two months after publication it is available to the public under an Attribution–Noncommercial–Share Alike 4.0 Unported Creative Commons License (<http://creativecommons.org/licenses/by-nc-sa/4.0>).

“ASCB®,” “The American Society for Cell Biology®,” and “Molecular Biology of the Cell®” are registered trademarks of The American Society for Cell Biology.

The PM is basically in a fluid liquid state (Singer and Nicolson, 1972) and probably contains more than 10,000 protein and lipid species (Holthuis and Menon, 2014). They interact with each other in complex ways (Simons, 2016), often forming a variety of nano- to microscale molecular complexes and domains with very broad ranges of lifetimes, from milliseconds to perhaps weeks (see Figure 5 of Kusumi et al., 2012b) (Simons and Sampaio, 2011), and sometimes with quite ambiguous boundaries with other domains/complexes, as exemplified by the presence of so-called lipid raft domains. The thermodynamic state of the PM has been proposed to be close to miscibility critical points exhibiting immense local compositional fluctuations, which might be essential for turning on cooperative switches to trigger important signaling processes and PM structural changes (Veatch and Keller, 2003; Honerkamp-Smith et al., 2008). This complicates the analyses of the system, because subtle variations in experimental conditions employed by different research groups could lead to quite dissimilar results.

Despite the VUCA of the PM as a system, in terms of its molecular composition two molecules stand out among all molecular species because of their abundance and essential roles in PM functions: cholesterol (CHOL) and actin. CHOL is the most common PM molecular species, representing ~35–45 mol% of all the PM lipids

(Subczynski *et al.*, 1991; Meer *et al.*, 2008; Simons and Sampaio, 2011). The actin “membrane skeleton,” which is the actin meshwork closely apposed to the PM cytoplasmic surface, and the cortical actin filament layers, with a thickness of ~25 nm (three to five layers of actin filaments) from the PM, are found virtually everywhere throughout the PM in eukaryotic cell lines (Morone *et al.*, 2006; Shirai *et al.*, 2017).

In this review, we advance the arguments that the CHOL- and actin-centered view of the PM can provide excellent perspectives for understanding a variety of key PM properties and functions, including those of “lipid rafts.” This year is the 50th anniversary of the publication of the fluid mosaic model by Singer and Nicolson (1972), which is undoubtedly still the most fundamental model for the PM structure and molecular dynamics. Even now, the fluid mosaic model is believed to represent the basic structure of the PMs of virtually all cells existing on Earth. Such universality is comparable to that of the double helical structure of DNA, although this point is often missed even in classrooms and textbooks. Just as many DNA functions are based on the DNA’s double helical structure, the various PM functions are enabled by the PM’s fluid mosaic structure.

However, to develop clearer synthetic understandings of how the PM performs its various functions, perhaps based on the PM VUCA, scientists have been modifying the fluid mosaic model to higher and finer levels by incorporating spatiotemporal heterogeneity (Manley *et al.*, 2008; Schubert and Wedlich-Söldner, 2015; Sezgin *et al.*, 2017; Jacobson *et al.*, 2019; Kalappurakkal *et al.*, 2020). For this purpose, in this article we propose that one of the useful ways to reach a synthetic understanding of the PM structure, dynamics, and functions is to regard the PM VUCA from the perspectives of CHOL and actin. We will explain that two major causes of PM spatiotemporal heterogeneity are brought about by CHOL and the parts of the cortical actin filaments directly bound to the PM (actin-based membrane skeleton). CHOL induces “raft domains” (defined later in this review), and the actin-based membrane skeleton induces the compartmentalization of the entire PM into 30–230-nm domains. Each raft domain basically exists within an actin-induced compartment.

CHOL-CENTERED VIEW OF THE PM

Strikingly nonlinear dependence of many signaling functions on the CHOL concentration in the PM

Mild CHOL depletion is a prevalent method to study the involvement of CHOL and so-called “lipid rafts” in biological processes of interest. However, the following key point is rarely considered.

The CHOL concentration in the PM of mammalian cells is generally around 35–45 mol% of total lipids. In normal CHOL-depletion experiments, the CHOL concentration is typically decreased by only 40% to 20–27 mol% (Green *et al.*, 1999; Surviladze *et al.*, 2001; Suzuki *et al.*, 2007b). For conciseness, in the following we state 40 and 25% to refer to the CHOL mole fractions in the PM before and after CHOL depletion, respectively. However, despite the presence of high concentrations (25 mol%) of CHOL remaining in the “CHOL-depleted” PM, many signaling reactions were shut down (we mostly consider events occurring at 37°C), as exemplified in the following reports: Green *et al.*, 1999; Sheets *et al.*, 1999; Abrami *et al.*, 2003; Seveau *et al.*, 2004; Monastyrskaya *et al.*, 2005; Vial and Evans, 2005; Hunter and Nixon, 2006; Suzuki *et al.*, 2007a,b; McGraw *et al.*, 2012; Korinek *et al.*, 2015; Ridone *et al.*, 2020; Wang *et al.*, 2021.

Therefore, the dependence of these signaling processes on the CHOL content is strikingly nonlinear: full reaction at 40 mol% CHOL and no reaction at 25 mol% CHOL. This clearly shows that these signaling reactions do not depend on simple interactions with single CHOL molecules but instead are enabled by the

domains/structures in the PM that are formed by cooperative interactions with CHOL in the presence of overall CHOL concentrations greater than 25 mol%.

Previous and currently prevalent “definitions” of raft domains

The special domains induced by CHOL are enriched in sphingomyelins. Accordingly, the idea that CHOL and sphingomyelins together form special lipid-based domains that stand out among the PM VUCA was born, and these domains were named “lipid rafts” about a quarter of century ago (Simons and Meer, 1988; Simons and Ikonen, 1997; Simons and Toomre, 2000; Harder and Simons, 1997; Rietveld and Simons, 1998). Although many researchers erroneously assumed that generally mild CHOL-depletion protocols removed most of the CHOL from the PM (rather than just ~40%), due to the experimental ease CHOL depletion became a very useful and popular method to examine the involvement of raft domains in various cellular events and molecular functions (Moran and Miceli, 1998; Fessler and Parks, 2011). Furthermore, this protocol was often coupled with biochemical purification methods to prepare lipid raft domains as aggregates of some fractions of lipid raft domains and raft-associated molecules, after extraction from various cells and tissues using nonionic detergents at 4°C (called detergent-resistant membranes or DRMs) (Brown and Rose, 1992). However, the interesting observations obtained by this approach failed to provide a clear definition of raft domains in the PM.

The lipid raft domain research field has long been plagued by the lack of a clear definition. If the raft domains had been visualized by microscopic methods, then the definition would have been easier. For example, the micronscale structures on the PM with lifetimes longer than several tens of seconds, such as synapses, adherens junctions, and clathrin-coated pits, and containing many (>10) copies of each key protein species could be defined simply, because they can be imaged by immunofluorescence and immunoelectron microscopy. The raft domains that could be visualized are limited to those that were enlarged and stabilized by external stimulation (often by non-physiologically strong stimulation) and by artificial cross-linking of raft-associated molecules. Therefore, the focus of interest in raft research has shifted to revealing whether the precursor raft domains that are triggered to become large, stabilized raft domains exist in quiescent cells before stimulation. If they do exist, what are the precursor domains, how do they behave, and how are they triggered to become enlarged, stabilized raft domains to perform cellular signaling? For such investigations, microscopic visualizations of precursor domains in the quiescent steady state must be made, but these observations have turned out to be enormously difficult.

At the 2006 Keystone Symposium on “Lipid Rafts and Cell Function,” lipid rafts were “defined” as “small (10–200 nm), heterogeneous, highly dynamic, sterol- and sphingolipid-enriched domains that compartmentalize cellular processes. Small rafts can sometimes be stabilized to form larger platforms through protein–protein interactions.” However, although this “definition” summarizes the general properties of raft domains in the PM quite well, it might not be very useful for research examining whether the observed molecules and events occur in raft domains and whether any raft domains are involved in the observed phenomena. As such, the older definitions of raft domains were often mixtures of definitions and properties, and usually difficult to apply to actual research.

Furthermore, the definition of raft domains often depended on the context in which they are considered. For example, in the biochemical context, the raft domains have long been defined as the DRM fraction. This definition has been useful for identifying the molecular candidates that might be involved in raft domains in the

PM. However, the largest problem is that DRMs could not be readily related to the actual raft domains in the PM, particularly those before stimulation (for example, in terms of their sizes, lifetimes, and distributions).

Therefore, a general definition of raft domains existing in the PM must be developed for the robust development of this research field. It must be useful for research in the future and in broad fields of biomedicine. In addition, the definition must include the cooperative interaction of CHOL with other molecules for the formation of raft domains, as explained in the preceding subsection.

Another key observation for defining raft domains in the PM

As described, many signaling reactions that depend on CHOL do not rely on simple interactions with single CHOL molecules, but instead are enabled by the CHOL-enriched domains/structures in the PM that are formed by cooperative interactions of CHOL with other constituent molecules. Such domains could be generated in the presence of overall CHOL concentrations greater than 25 mol% in the PM.

Another critically important observation was made using giant plasma membrane vesicles (GPMVs) or PM spheres, formed by PM blebbing after the dissociation of the actin-based membrane skeleton from the PM cytoplasmic surface. Upon cooling to $\sim 10^\circ\text{C}$, GPMVs generally have two coexisting and complementary micron-scale *liquid* domains (Baumgart *et al.*, 2007; Lingwood *et al.*, 2008; Levental *et al.*, 2009, 2010; Johnson *et al.*, 2010). These domains exhibit the characteristics of the liquid-ordered and liquid-disordered phases (Lo- and Ld-phases, respectively) found in artificial giant unilamellar vesicles (GUVs) with the proper lipid compositions, typically a ternary 1:1:1 mixture of long, saturated phosphatidylcholine (PC) or sphingomyelin, CHOL, and unsaturated PC, at temperatures below 37°C (for the Lo- and Ld-phases, see the next subsection, *Detailed explanation 1*; Figure 1, A–C).

Importantly, these results showed that the PM is capable of undergoing large-scale phase separations into Lo-phase-like and Ld-phase-like domains, when the actin-based membrane skeleton is removed and the temperature is lowered to $\sim 10^\circ\text{C}$. Interestingly, after mild partial CHOL depletion, the Lo-phase-like microscale domains could not be induced upon cooling to 10°C (Johnson *et al.*, 2010), suggesting that the presence of overall CHOL concentrations of 25 mol% or more in the PM is essential for producing Lo-phase-like domains in GPMVs at $\sim 10^\circ\text{C}$. This requirement is essentially the same as that for many PM signaling functions, as described in preceding paragraphs, as well as for the induction of Lo–Ld-phase separation in GUVs (see Section 4 of Kusumi *et al.*, 2020).

Detailed explanation 1: Lo- and Ld-phases in GUVs and biological membranes

Readers familiar with Lo- and Ld-phases should skip this subsection. They can do so without losing track of the main flow of this article.

The liquid properties of biological membranes are induced by the thermally driven conformational changes of individual single bonds in the fatty acyl chains of phospholipids and sphingolipids ($-\text{CH}_2-\text{CH}_2-$), from the more stable *trans* conformation to either one of the two *gauche* conformations ($[+]\textit{gauche}$ and $[-]\textit{gauche}$) (Figure 1A). The *gauche* conformations induce a 60° bend in the acyl chain, which prevents the lipid molecules from being packed closely in the membrane. The acyl chain order, which is often defined by the spread (distribution) of the angles of the C–C bonds in each $-\text{CH}_2-\text{CH}_2-$ group relative to its average orientation (averaged over all the molecules and also over the characteristic time span for the obser-

vation method used), is generally coupled with how well the acyl chains are packed in the membrane: higher packing generally means higher acyl chain order (fewer *gauche* conformations).

The double bond in a fatty acyl chain works like a fixed *gauche* bond; that is, a mandatory 60° bend in the acyl chain (although their exact conformations are different) (Figure 1B). Therefore, the membranes containing lipids with one or two unsaturated fatty acyl chains (unsaturated lipids) are less packed, blocking the solidification of the membrane, which is important for organisms living in cold environments.

In artificial membranes, like GUVs, in the absence of CHOL the acyl chain packing and order are low at higher temperatures and thus constituent lipid molecules can undergo rapid translational diffusion. Thermodynamically, such membranes are in the liquid-disordered phase (Ld-phase), which was so named because lipid molecules undergo Brownian diffusion in the membrane (a characteristic of the liquid) and the acyl chains are disordered.

The effects of CHOL on the membrane structure and dynamics in GUVs can be understood in terms of three types of CHOL–acyl chain interactions.

1. When an acyl chain is located adjacent to a CHOL molecule, due to the rigid tetracyclic skeletal structure of CHOL, the *gauche* conformation is suppressed, thus inducing more *trans* conformations and increasing the acyl chain packing (Figure 1B). Therefore, the presence of CHOL generally enhances the acyl chain order in membranes in the Ld-phase.
2. Upon lowering the temperature, because the presence of CHOL induces defects in the alignment of acyl chains, the packing in the solid phase is lower. Namely, CHOL enhances alkyl chain *disorder* in membranes in the solid phase (where acyl chains are quite well aligned and no translational diffusion of lipids occurs).
3. CHOL and unsaturated acyl chains tend to exclude each other because the forced 60° bend at the double bond prevents the acyl chain from following along the rigid tetracyclic skeletal structure of CHOL (called “lateral non-conformability”; Kusumi *et al.*, 2005) (Figure 1B).

At sufficiently high temperatures, GUVs composed of ternary mixtures of >25 mol% CHOL and saturated and unsaturated lipids form the Ld-phase membrane. Upon cooling, unsaturated lipids are excluded from the CHOL's rigid tetracyclic backbone surface (Interaction 3), where saturated lipids must come in and interact. Under certain conditions, such CHOL effects induce phase-separated membranes consisting of the Ld-phase domain containing a high content of unsaturated lipids and lower amounts of saturated lipids with smaller amounts of CHOL and the other phase domain mostly consisting of CHOL and saturated lipids with small amounts of unsaturated lipids (Figure 1C). The latter membrane domain exhibits higher acyl chain order compared with the Ld-phase domain, due to the interaction of CHOL with saturated fatty acyl chains (Interaction 1), but the packing is less dense than that in the solid phase due to the lower alignment of saturated lipids next to CHOL (Interaction 2), allowing lateral diffusion of the constituent molecules (liquid property). Accordingly, the latter domain tends to be in the liquid-ordered phase (Lo-phase domain).

The thermodynamic phase can be strictly defined for GUVs comprising a few defined lipid species. However, for membranes composed of many molecular species, like biological membranes, because the phase cannot be defined readily we call the disordered and ordered liquid states “Ld-phase-like” and “Lo-phase-like” or simply “Ld-like” and “Lo-like” states, respectively. Some authors

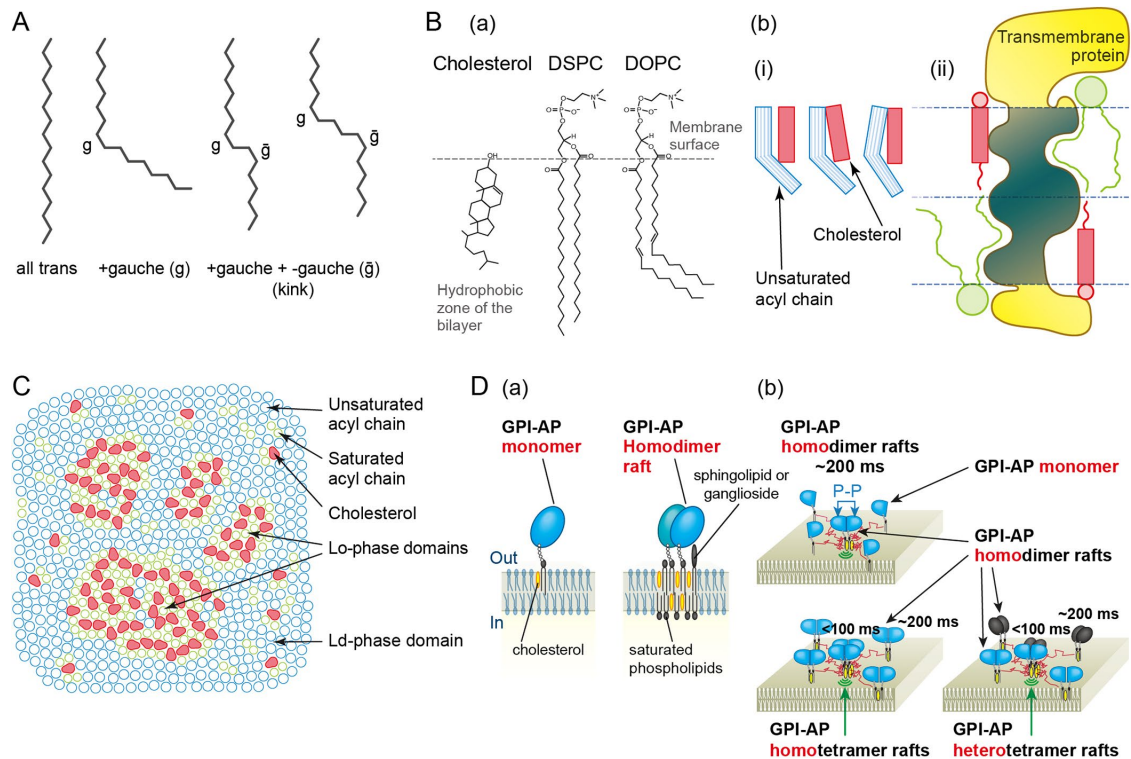


FIGURE 1: Key molecular interactions for the formation of various raft domains. (A) All *trans* conformations and two *gauche* conformations ([+]*gauche* and [−]*gauche*) of the alkyl chains (−CH₂−CH₂−)_n. The *gauche* conformation is induced by the rotation around a single bond between two adjacent CH₂ groups. The *gauche* conformation induces 60° bend in the acyl chain. Because the inclusion of a single *gauche* conformation in a chain is quite unfavorable for the acyl chain packing in the membrane (and thus energy), the second *gauche* conformation occurs frequently near the first *gauche* conformation. Such double *gauche* conformations are called kinks. The formation of *gauche* conformations (rotation around single bonds) and the rapid interconversions between the *trans* and *gauche* conformations are the fundamental causes for inducing fluidity (liquid-like property) of the PM. (B) (a) Chemical structures of CHOL and representative saturated and unsaturated phospholipids frequently used in the studies of GUVs. Saturated lipid: L- α -distearoylphosphatidylcholine (DSPC). Unsaturated lipid: L- α -dioleoylphosphatidylcholine (DOPC). When saturated lipids, such as DSPC, are located next to a CHOL molecule, due to the rigid tetracyclic skeletal structure of CHOL, the *gauche* conformations of the acyl chain between the carbonyl carbon C1 (−COO) and the 12th carbon C12 are suppressed, inducing more *trans* conformations and increasing the acyl chain packing. However, unsaturated lipids, such as DOPC, have at least a single *cis* bond between C9 and C10, which induces a mandatory 60° bend there. The mandatory 60° bend of the unsaturated acyl chain causes steric problems when it is next to a CHOL molecule. (b) (i) Schematic figure showing three possible configurations for placing CHOL and an unsaturated chain next to each other, indicating that good packing of these two structures is difficult. This is due to the mismatch (nonconformability) between the mandatory 60° bend at the double bond in the unsaturated acyl chain and the rigid tetracyclic skeletal structure of CHOL (magenta rectangles). Therefore, CHOL and unsaturated acyl chains tend to exclude each other, which is called lateral nonconformability, and CHOL tends to associate with saturated lipids if given the choice. Such accommodating and nonconformable interactions of CHOL with saturated and unsaturated lipids, respectively, are the main cause of phase separation in the ternary mixtures of CHOL, saturated lipids, and unsaturated lipids. (ii) The rigid ring structure of CHOL, located adjacent to the rough surface of the TM domain of the TM protein (induced by the protruding hydrophobic side chains of the amino acids in the membrane), would generate vacant pockets (packing defects). In this manner, CHOL is excluded from the first annulus of most TM proteins. Therefore, the CHOL-based raft domains are excluded from the PM compartment boundaries due to their exclusion from the rows of the TM picket proteins anchored to and aligned along the actin-based membrane skeleton fence. The TM proteins with raft affinities are expected to be well miscible with CHOL molecules. (C) Schematic snapshot drawings of the phase-separated GUV membrane, made of saturated lipids, such as DSPC, and unsaturated lipids, such as DOPC, and CHOL (top view). Open circles represent acyl chains (saturated chain in green and unsaturated chain in cyan; two chains form a lipid molecule), and solid magenta structures indicate CHOL molecules. The regions enriched in saturated lipids and CHOL represent the Lo-phase domains, and those enriched in unsaturated lipids represent the Ld-phase domains. Note that Lo-phase domains additionally contain smaller amounts of unsaturated lipids and Ld-phase domains additionally contain smaller amounts of saturated lipids and CHOL. Fluorescence microscopy observations might suggest the presence of submicronscale–micronscale Lo-phase domains, but they might actually represent the membrane regions enriched in nanoscale (several to several tens of nanometers) Lo-phase domains. (D) (a, left) Schematic model of a GPI-AP. The protein moiety is linked to phosphatidylinositol (PI), a phospholipid, via a short glycochain. The glycosylated PI (GPI) anchors the protein moiety to the PM outer leaflet. The monomeric GPI-AP can associate with raft domains, but its affinity is low (left). (a, right) Schematic model of the metastable GPI-AP homodimer rafts, which are formed by specific

call these states of the biological membranes the Ld- and Lo-phases, but readers should know that this would be a loose terminology.

In artificial membranes consisting of only CHOL and unsaturated lipids, CHOL molecules form transient clusters (oligomers), probably due to exclusion from the space around unsaturated acyl chains. Such CHOL clusters form and disperse continually with a lifetime of the order of 0.1–1 ns (Subczynski *et al.*, 1990).

The occurrence of Interaction 1 increases the number of *trans* configurations in the acyl chains and enhances the lipid packing, which would make the Lo-phase domains thicker than the Ld-phase domains. Cryoelectron microscopy/tomography directly visualized the membrane thickness in the Lo-phase domain to be greater than that in the Ld-phase domain in GUVs (Cornell *et al.*, 2020; Heberle *et al.*, 2020). The thickness distribution of GPMVs suggested the nanoscale lateral heterogeneities (Heberle *et al.*, 2020).

Revised definition of raft domains

On the basis of the argument developed in the preceding section (Lo-phase-like and Ld-phase-like domains coexist in the PM of living cells), as the *definition* of raft domains in the PM, we propose the following: “Raft domains in the PM are Lo-phase-like, CHOL-centered molecular complexes/domains formed by cooperative interactions of CHOL with saturated acyl chains as well as unsaturated acyl chains and transmembrane (TM) proteins.” This definition represents the fundamental mechanism for the formation of raft domains in the PM: the cooperative interactions due to saturated acyl chains’ weak multiple accommodating interactions with CHOL and, importantly, the low miscibility of CHOL with unsaturated acyl chains and TM proteins (collectively called “raft-lipid interactions”), which occur in the presence of >25 mol% CHOL. The latter half of this definition is quite different from previous definitions in that it includes CHOL exclusion from the sites adjacent to unsaturated lipids and TM domains. For details about the interactions of CHOL with saturated and unsaturated acyl chains and TM proteins, see the preceding subsection, *Detailed explanation 1*, and Figure 1, A–C.

In developing this new definition, we wanted to make it very general but also very strong. Here, the critical molecular species to form raft domains are only CHOL and molecules containing saturated and unsaturated acyl chains. The definition is based on CHOL’s cooperative interactions with saturated acyl chains (accommodating) as well as with unsaturated acyl chains and proteins’ TM domains (nonconformable). These accommodating and nonconformable interactions together induce cooperative interactions. Previously, the “lateral nonconformability” between CHOL and unsaturated acyl chains was often neglected, making the meaning of the cooperativity unclear.

This concept is close to the mechanism for the formation of the Lo-phase in the artificial ternary mixtures of CHOL, lipids with long

saturated acyl chains, and lipids with unsaturated acyl chains, but in the definition of raft domains the Lo-phase formation is unnecessary. The key is not the formation of the phase, but the cooperative interactions. The cooperativity might start with only a few molecules that are included in raft domains (such as homodimer rafts of glycosylphosphatidylinositol-anchored proteins [GPI-APs] and CHOL; Suzuki *et al.*, 2012) and the surrounding unsaturated chains (although the Lo-phase might be defined for a molecular assembly of ≈ 10 molecules surrounded by unsaturated lipids; Kusumi *et al.*, 2020).

Because this definition is based on the fundamental mechanism for the formation of raft domains, it should be applicable and useful for testing molecular complexes in the PM found in diverse biomedical fields. The application of this definition to experimental research is described in the next subsection, *Practical guide for studying raft domains in the PM based on the new raft definition*.

It is critically important to realize that the interactions of individual molecules in and near the CHOL-centered raft domains are transient and weak. The sum of many weak accommodating and nonconformable interactions is the key for raft formation and for explaining the physical properties of raft domains. Therefore, all of the involved molecules in and around the raft domains should dynamically undergo thermal diffusion, readily moving in and out of raft domains (Kenworthy *et al.*, 2004; Suzuki *et al.*, 2007a,b, 2012). This is consistent with the concept that the thermodynamic state of the PM is close to miscibility critical points exhibiting immense local compositional fluctuations (Veatch and Keller, 2003; Honerkamp-Smith *et al.*, 2008). Although the space scales of the fluctuation were considered to be quite long, ≈ 20 nm (Veatch and Keller, 2003; Honerkamp-Smith *et al.*, 2008), the experimental data about GPI-AP homodimer rafts suggest that the sizes of raft domains can be as small as a few nanometers (Suzuki *et al.*, 2012; Tiwari *et al.*, 2018).

A cautionary remark is necessary here. Lo-phase-like domains that do not involve CHOL might exist in the PM. Fluorescence lifetime measurements, using environmentally sensitive membrane dyes that report the degree of lipid packing, suggested that $\sim 76\%$ of the liquid is in the “ordered” state, although the exact meaning of the ordered state must be further clarified (Owen *et al.*, 2012).

Practical guide for studying raft domains in the PM based on the new raft definition

This definition of raft domains would be convenient to use for future research in a variety of biomedical fields. On the basis of the definition, we propose the following three criteria for determining whether the molecule of interest preferentially partitions into and functions in raft domains in the PM.

homoprotein interactions (P-P) and stabilized by raft-lipid interactions (which prolong the lifetime of homodimers). All GPI-APs examined thus far form metastable homodimer rafts with lifetimes on the order of ~ 200 ms. (b) GPI-AP homodimer rafts merge to form GPI-AP tetramer rafts by raft-lipid interactions (green ripples), rather than protein–protein interactions. The tetramer raft lifetimes are shorter (~ 100 ms) than the homodimer raft lifetimes. When GPI-AP homodimer rafts of the same GPI-AP species merge, they form homotetramer rafts, and when GPI-AP homodimer rafts of different GPI-AP species merge, they form heterotetramer rafts. Such flexibility of protein species in tetramer rafts is possible because the merging is mediated by raft-lipid interactions, rather than protein–protein interactions. These results suggest that the formation of metastable GPI-AP homodimer rafts represents the first step in the formation of raft domains and that the GPI-AP homodimer rafts are one of the basic units for generating greater raft domains. The formation of GPI-AP tetramer rafts would be the second step for the formation of greater raft domains. The next step required for the formation of greater raft domains is the stabilization of greater raft domains, which would be triggered by signaling, including the pathways of Src-family kinases and trimeric G proteins, and probably by interactions with active actomyosin systems.

1. Preferential partitioning into Lo-like domains in GPMVs at 10°C;
2. Preferential partitioning into detergent-resistant membranes using Triton X-100 at 4°C;
3. Greatly reduced/altered function after mild CHOL depletion, and recovery of the original function soon after CHOL replenishment.

Basically, all three criteria should be satisfied for a molecule to be categorized as a raft-associated molecule. This is because each of these criteria is not based on the all-or-none law, but the preference addresses a quantitative difference and thus higher probability. Furthermore, these criteria are based on molecular behaviors in very different contexts/conditions. Therefore, we think that satisfying all three of these criteria is important.

Previously, we proposed another criterion, "Preferential partitioning into the Lo-phase domains in Lo-Ld-phase-separated GUVs after reconstitution at 25°C," but we replaced it with the third criterion described here because the use of GUVs requires extensive experiments and might not be practical in various research projects (for details, see Sections 10 and 13 of Kusumi *et al.*, 2020). We believe that this third criterion effectively represents the definition and would be more practical for applications to molecular cell biological studies. Note that CHOL repletion experiments must be performed to confirm that the effect of CHOL depletion was directly induced by the loss of raft domains, rather than artifactual side effects of CHOL depletion (Kenworthy *et al.*, 2004; Suzuki *et al.*, 2007a,b, 2012), although CHOL repletion experiments are rarely performed. For example, because acute CHOL depletion could induce actin reorganization and reduce the mobilities of PM molecules, its effect can be strong and broad in various assays (Kwik *et al.*, 2003). However, because this effect does not disappear for 12–24 h after CHOL repletion (Kwik *et al.*, 2003), if CHOL repletion quickly restores the molecular functions and behaviors before CHOL depletion, then the CHO-depletion effect is likely induced by the loss of raft domains.

To assess the involvement of raft domains in biological events/phenomena of interest in the live-cell PM, we recommend examinations of the recruitment/involvement of GPI-APs (Suzuki *et al.*, 2012) and the recently developed fluorescent analogues of sphingomyelin and gangliosides, GM1, GM2, GM3, and GD1b (Komura *et al.*, 2016; Kinoshita *et al.*, 2017; Arumugam *et al.*, 2021); for an extensive summary, see Table 4 of Kusumi *et al.* (2020). Note that virtually all fluorescent ganglioside and sphingomyelin analogues used before these publications preferentially partitioned into Ld domains (Sezgin *et al.*, 2012a) and thus could not and will not serve as raft markers (these studies tended to erroneously arrive at wrong conclusions). Protein toxin-based CHOL and sphingomyelin probes could also be used, but due caution is required because their affinities tend to be low and affected by their environment (readers interested in the protein probes for CHOL and sphingomyelins, see the next subsection, *Detailed explanation 2*).

Because the sizes of PM raft domains in quiescent cells might be on the order of 2–20 nm (Kusumi *et al.*, 2020), the recruitment and colocalizations would be better observed by employing single-molecule imaging methods (Komura *et al.*, 2016; Kinoshita *et al.*, 2017; Arumugam *et al.*, 2021). When single-molecule localization microscopy, such as PALM/STORM, is utilized, note that simply gathering images would not be very useful. Instead, the spatial correlations and colocalizations of individual molecules of interest (fluorescent spots) with individual molecules of the raftophilic lipid probes (fluorescent spots) must be obtained (Stone and Veatch, 2014; Pigeon *et al.*, 2016; Simoncelli *et al.*,

2020); for the method to circumvent the overcounting problem, see Arnold *et al.* (2020). However, because lipid probes cannot be chemically fixed (Tanaka *et al.*, 2010), observations in living cells, using fast data acquisition frame rates, would be preferable (Fujiwara *et al.*, 2021b).

For further understanding of raft domains, excellent recent reviews, which have not been cited thus far in this article, are available. For example, refer to Sevcsik and Schütz (2016), Levental *et al.* (2020), and Regen (2020).

Recently, using protein toxin-based CHOL probes, the existence of three distinct CHOL pools in the PM outer leaflet has been found (Das *et al.*, 2014; Endapally *et al.*, 2019). Their relationships with raft domains are not clear, but the 2–20-nm-scale raft domains could be classified into those that do or do not contain sphingomyelin. These three CHOL pools are summarized in *Detailed explanation 3*.

Detailed explanation 2: Protein-based CHOL probes

Readers who are not interested in this subject matter can skip this subsection without losing track of the main flow of this article.

CHOL probes based on bacterial and mushroom toxins (proteins) have recently been developed. The most popular probes employ the carboxy-terminal ~13-kDa domain, referred to as domain 4 (D4), derived from perfringolysin O (PFO) (Ohno-Iwashita *et al.*, 1990; Nakamura *et al.*, 1995; Shimada *et al.*, 2002) or anthrolysin O (ALO) (Bourdeau *et al.*, 2009; Farrand *et al.*, 2010). D4H, the D434S mutant, exhibited higher affinity to CHOL (Johnson *et al.*, 2012; Maekawa and Fairn, 2015). Liu *et al.* (2017) developed a ratiometric fluorescence imaging method that allows simultaneous *in situ* CHOL quantifications in both PM leaflets, using four orthogonal CHOL sensors, which facilitate the selection of probes with proper affinities for each experiment (Cho *et al.*, 2022). Although these probes turned out to be extremely useful (Zhang *et al.*, 2018; Cho *et al.*, 2022), the results obtained with them should be interpreted carefully because their binding might be sensitive to particular lipid-lipid interactions, phase states, and masking by the binding of CHOL's physiological interaction partner proteins (Maxfield and Wüstner, 2012; Courtney *et al.*, 2018).

Probes based on mushroom toxins, ostreolysin A (OlyA) and nakanori, which bind only to the sphingomyelin-CHOL complex, have also been developed (Ota *et al.*, 2013; Das *et al.*, 2014; Skočaj *et al.*, 2014; Makino *et al.*, 2017; Endapally *et al.*, 2019).

Structural and biochemical analyses showed that the conformation of CHOL-bound sphingomyelin is different from that of free sphingomyelin (Endapally *et al.*, 2019). The E69A and E69S mutants of OlyA can bind to both free sphingomyelin and sphingomyelin complexed with CHOL and thus could be used as sphingomyelin probes (another powerful sphingomyelin probe is lysenin [Yamaji *et al.*, 1998; Tomishige *et al.*, 2021]). Interestingly, the E69G mutant exhibited specificity to the sphingomyelin-CHOL complex, whereas the E69N and E69D mutants failed to bind either form of sphingomyelin.

The D4 domain of PFO (and Y181A, called PFO*, used at 4°C; at 37°C, like PFO, PFO* forms pores in the PM) is very useful. It binds to free CHOL, but not the sphingomyelin-CHOL complex. Together with OlyA, which binds only to the sphingomyelin-CHOL complex, three distinct CHOL pools in the PM outer leaflet were identified (Das *et al.*, 2014; Endapally *et al.*, 2019). They are the D4-accessible (~16 mol% CHOL vs. total lipid), sphingomyelin-sequestered (~15 mol%), and essential (~12 mol%) CHOL pools (see *Detailed explanation 3*, the next subsection). The essential CHOL pool is thus termed because its depletion causes cells to round up

and dissociate from the substrate. This pool is protected from D4 and OlyA binding and could be removed only by a treatment with 2-hydroxypropyl- β -cyclodextrin (and methyl- β -cyclodextrin) after the D4-accessible and sphingomyelin-sequestered pools were first depleted (Das *et al.*, 2014).

Detailed explanation 3: Three distinct CHOL pools exist in the PM outer leaflet

Readers who are not interested in this subject matter should skip this subsection and directly move to the next subsection.

Three distinct CHOL pools in the PM outer leaflet were identified (Das *et al.*, 2014; Endapally *et al.*, 2019) using toxins that bind to CHOL in different states. The carboxy-terminal ~13-kDa domain of the bacterial toxin PFO, referred to as domain 4 (D4), binds only to free CHOL, and the mushroom toxin OlyA binds only to the sphingomyelin-CHOL complex (see *Detailed explanation 2* for the protein-based CHOL probes). The three distinct CHOL pools are called the D4-accessible (~16 mol% CHOL vs. total lipid), sphingomyelin-sequestered (~15 mol%; OlyA binding), and essential (~12 mol%) CHOL pools. The essential CHOL pool is thus termed because its depletion causes cells to round up and dissociate from the Petri dish. This pool is protected from D4 and OlyA binding and could be removed only by a treatment with 2-hydroxypropyl- β -cyclodextrin (and methyl- β -cyclodextrin) after the accessible and sphingomyelin-sequestered pools are first depleted (Das *et al.*, 2014).

The D4-accessible and sphingomyelin-sequestered CHOL pools appear only when the CHOL contents in the PM are greater than 35 and 25 mol%, respectively. Clarification of the relationships of these three CHOL pools with the Lo-Ld-phases in GUVs and GPMVs is the next key issue. The D4-accessible pool is involved in many cellular processes, including hedgehog signaling (Kinnebrew *et al.*, 2019), resistance to cytolysin formation (Zhou *et al.*, 2020), and blocking bacterial infection (Abrams *et al.*, 2020). The biological functions of the sphingomyelin-sequestered CHOL pools are barely known, but recently their function during the initial stages of the influenza virus (IFV) entry via clathrin-coated structures was reported (Tang *et al.*, 2022). The sphingomyelin-CHOL complex nanodomain is recruited to the IFV-containing clathrin-coated structure, and then formin-binding protein 17 (FBP17), a membrane-bending protein that activates actin nucleation, is recruited to this sphingomyelin-CHOL complex, facilitating the neck constriction of the IFV-containing clathrin-coated structure.

Detailed explanation 4: GPI-APs occupy an important position in raft research

Readers who are familiar with the research fields of raft domains including GPI-APs can skip this subsection without losing track of the main flow of this article.

In the human genome, more than 150 protein species have been identified as GPI-APs, in which the protein moieties located at the PM extracellular surface are anchored to the PM by way of GPI, a phospholipid (Kinoshita and Fujita, 2015; Figure 1Da). Most of the GPIs of GPI-APs contain two saturated fatty acyl chains of C18 and longer. Very small fractions of GPIs contain an unsaturated C24:1 acyl chain, but interestingly, the double bond exists near the terminal methyl group (Kusumi *et al.*, 2004, 2020). Therefore, their interactions with CHOL would be close to those of saturated acyl chains. This suggests that GPI-APs might be involved in the formation and functions of raft domains. Indeed, in raft research, GPI-APs occupy an important position.

First, all GPI-APs examined thus far appear to satisfy all three criteria described in the subsection *Practical guide for studying raft*

domains in the PM based on the new raft definition to be categorized as raft-associated molecules. For example, for "1) preferential partitioning into Lo-like domains in GPMVs at 10°C," see Sengupta *et al.* (2008) and Sezgin *et al.* (2012b); for "2) preferential partitioning into detergent-resistant membranes using Triton X-100 at 4°C," see Brown and Rose (1992) and Suzuki *et al.* (2012); and for "3) greatly reduced/changed function after mild CHOL depletion, and recovery of the original function upon CHOL replenishment," see Suzuki *et al.* (2007a,b, 2012).

Second, GPI-APs have played historically important roles in raft research. GPI-APs were key molecules for developing the use of DRMs in raft research (Brown and Rose, 1992), examining possible raft involvement in polarized sorting and transport (Dotti *et al.*, 1991; Fiedler *et al.*, 1993; Zurzolo and Simons, 2016), and investigating raft involvement in receptor signaling (Stulnig *et al.*, 1997; Moran and Miceli, 1998). Gangliosides and sphingomyelins might be extensively associated with raft domains, but the raft functions involved in signaling could be better studied using GPI-APs. As such, GPI-APs have been extensively used as representative molecular species located and functioning in raft domains in the PM and have facilitated important conceptual advances about raft domains in the PM. One of the key characteristics of GPI-APs is that by replacing the GPI-anchoring chain with the transmembrane domain of a nonraftophilic single-pass transmembrane protein, without CHOL depletion, their raft involvement can be totally suppressed, and thus this property allows us to investigate the raft involvement of GPI-AP-related functions without CHOL depletion (Varma and Mayor, 1998; Suzuki *et al.*, 2012).

Third, many GPI-APs are receptors and trigger signaling pathways involving tyrosine kinases, phospholipase C, and Ca²⁺ (Štefanová *et al.*, 1991; Green *et al.*, 1999; Sheets *et al.*, 1999; Abrami *et al.*, 2003; Seveau *et al.*, 2004; Monastyrskaya *et al.*, 2005; Vial and Evans, 2005; Hunter and Nixon, 2006; Suzuki *et al.*, 2007a,b; McGraw *et al.*, 2012; Korinek *et al.*, 2015; Ridone *et al.*, 2020; Wang *et al.*, 2021). Because GPI-APs are associated with raft domains, they are often chosen to study the mechanisms by which raft domains work for signal transduction.

Meanwhile, the GPI-anchored structure is almost paradoxical for receptors because, although it relays the signal from the outside environment to the inside of the cell, it spans only halfway through the membrane (Figure 1Da). The involvement of "raft domains" has been implied in the transbilayer signaling by the GPI-AP receptors, but exactly how raft domains or raft-based lipid interactions participate in the transbilayer signal transduction of GPI-AP receptors remains unknown, despite extensive research (in addition to the references cited in the preceding paragraph, we suggest the following references for further reading: Omidvar *et al.*, 2006; Paulick and Bertozzi, 2008; Lingwood and Simons, 2010; Eisenberg *et al.*, 2011; Fessler and Parks, 2011; Kusumi *et al.*, 2014; Raghupathy *et al.*, 2015).

Fourth, as described, all GPI-APs examined thus far form metastable homodimer rafts (Suzuki *et al.*, 2012). These metastable homodimer rafts are considered to be one of the basic raft "units" that will form greater raft domains (Suzuki *et al.*, 2012), and thus the generation of such homodimer rafts would constitute the first fundamental step in raft domain formation (Figure 1Db).

As such, GPI-APs occupy a critical and unique position in raft research. Therefore, in this review we will extensively discuss the behaviors and functions of GPI-APs.

Metastable homodimer rafts of GPI-APs are one of the basic units for raft formation and function

As summarized in the preceding subsection, GPI-APs have occupied very special positions in raft research (Figure 1D, a and b).

Using GPI-APs, Suzuki *et al.* (2012) identified one of the most fundamental steps, and probably the first step, for the formation of raft domains. This is based on the finding that essentially all molecular species of GPI-APs, including CD59, DAF, Thy-1, and Prion Protein, form dynamic, *metastable homodimer rafts*, with lifetimes on the order of 200 ms (Figure 1Db) (Suzuki *et al.*, 2012; Tiwari *et al.*, 2018). The formation of GPI-AP homodimer rafts requires ectodomain protein homointeractions, which are stabilized by raft-lipid interactions. In the context of raft studies, attention was typically paid only to raft-lipid interactions, but here, specific protein–protein interactions were found to be critical for the formation of homodimer rafts (because GPI-APs form homodimers rather than heterodimers, the protein interaction is very specific). Because all GPI-APs examined thus far form metastable homodimer rafts, these structures are considered to be one of the common basic characteristics of GPI-APs. These observations were made possible by advanced single-fluorescent-molecule imaging. Meanwhile, the crystal structure of a GPI-AP dimer, human urokinase-type plasminogen activator receptor (uPAR), was recently reported and revealed enormous conformational changes of the dimer as compared with the monomeric structure (Yu *et al.*, 2022). Such extensive conformational changes might also occur to induce metastable homodimers of other GPI-APs.

The formation of metastable GPI-AP homodimer rafts might be the first step for the formation of any raft domains containing GPI-APs, because greater raft domains containing GPI-APs, such as GPI-AP trimer rafts and tetramer rafts, are generated by the merging of GPI-AP homodimer rafts with a GPI-AP monomer or another GPI-AP homodimer raft, indicating that GPI-AP homodimer rafts are the major building blocks for the production of greater raft domains (Figure 1Db) (Suzuki *et al.*, 2012). Furthermore, the merging is likely induced by raft-lipid interactions, rather than protein–protein interactions, because GPI-AP *hetero*-trimer and tetramer rafts are formed as readily as *homo*-trimer and tetramer rafts and their lifetimes are about the same (not much involvement of protein–protein interactions for the merging; Figure 1Db) and also because the merging is CHOL dependent (Suzuki *et al.*, 2012). Because these greater GPI-AP-containing rafts are formed by raft-lipid interactions, they can have flexible GPI-AP compositions. Therefore, we consider the formation of GPI-AP homodimer rafts as the first step for the formation of raft domains containing GPI-APs, and the merging of GPI-AP homodimer rafts by raft-lipid interactions is the second step. This further means that the results of many studies of GPI-APs might have to be reinterpreted, because what the authors assumed to be GPI-AP monomers might have actually been GPI-AP homodimer rafts.

Using CD59, Suzuki *et al.* (2012) also found that the homodimer rafts are the basic units for inducing cytoplasmic signals after the membrane attack complex binds to CD59. Suppression of the homodimer raft formation, using a mutant CD59 in which CD59's GPI anchor was replaced by the TM domain of the nonraft LDL receptor, made the cytoplasmic Ca²⁺ mobilization triggered by binding of the membrane attack complex to CD59 much smaller and slower. These results further indicate that the GPI-AP's metastable homodimer rafts are one of the basic building blocks for the formation of greater *functional* raft domains containing GPI-APs.

We raise the possibility that this process, in which the homodimers induced by specific molecular interactions form the cores for producing basic metastable homodimer raft domains, might also be true for other key raft-forming molecules, such as glycosphingolipids and sphingomyelins. We further consider that these various homodimer rafts are the basic fundamental units for building most of the greater raft domains in the PM and that the greater raft domains

are generated by the merging of these basic raft units by raft-lipid interactions.

Submicronscale–micronscale GPI-AP-raft-enriched domains

In single-molecule imaging studies, the number density of the observed (fluorescently labeled) GPI-APs in the PM is ~ 0.6 copies/ μm^2 . This is the condition where single molecules and the interactions of single molecules in the PM could readily be observed. However, such expression levels are not suitable to observe greater raft domains.

Mayor's group employed cells expressing GPI-APs with a total number density of ≈ 400 copies/ μm^2 , expression levels $\approx 700\times$ higher than those used by Suzuki *et al.* (2012) (still within the physiological range), and observed GPI-AP oligomers and assemblies by using time-resolved Förster resonance energy transfer (FRET) imaging. Sharma *et al.* (2004) showed that 20–40% of GPI-APs exist in clusters smaller than *hetero*-pentamers (nondiscrimination of the protein species), with the remaining 60–80% being monomers (which might actually be homodimer rafts, because the time-resolved FRET method is not sensitive enough to detect homodimers).

Mayor and colleagues further found that the submicronscale–micronscale rafts containing heteromixtures of GPI-APs form in a manner depending on ATP and actin filaments (Goswami *et al.*, 2008; Zanten *et al.*, 2009, 2010; Komura *et al.*, 2016; Kinoshita *et al.*, 2017; Arumugam *et al.*, 2021). Because the formation of GPI-AP homodimer, trimer, and tetramer rafts does not depend on actin filaments (Suzuki *et al.*, 2012; Tiwari *et al.*, 2018), these results together indicate that active processes involving actin filaments may be important for the formation of much greater submicronscale–micronscale rafts containing heteromixtures of GPI-APs (Plowman *et al.*, 2005; Goswami *et al.*, 2008; Gowrishankar *et al.*, 2012; Raghupathy *et al.*, 2015). We propose that these greater rafts would consist of GPI-AP homodimer rafts that are weakly glued together by raft-lipid interactions, which might associate with the actin filaments located on the PM cytoplasmic surface and thus become stabilized. Nevertheless, the GPI-AP homodimer rafts in such actin-induced submicronscale–micronscale rafts would be continually (all the time) exchanging with those existing as GPI-AP homodimer rafts and monomers in the bulk PM.

The submicronscale–micronscale rafts might not be continuous entities (Heberle *et al.*, 2010, 2013, 2020; Pathak and London, 2011; Bhatia *et al.*, 2014, 2016; Cornell *et al.*, 2020). They are detected by optical microscopy, and, considering their limited spatial resolutions, these “rafts” might simply be the PM regions where true smaller raft domains are concentrated by the actomyosin mechanical system. However, when the raft domains are concentrated, they would fuse readily. However, the decomposition rates should not be affected by the concentration. Therefore, in these raft-enriched domains, extensive and rapid fusing and splitting of raft domains must be occurring continually. We think that these raft-enriched domains are extremely interesting in terms of their functions and the dynamic mechanisms by which they are formed.

ACTIN-CENTERED VIEW OF THE PM

Dynamic actin meshwork partitions the PM into ≈ 100 -nm compartments

Cortical actin filament layers, with a thickness of ≈ 25 nm from the PM cytoplasmic surface and representing three to five overlaid actin filaments, are found virtually everywhere throughout the PM cytoplasmic surface in eukaryotic cells, except for newly forming thin lamellipodial and filopodial regions (Morone *et al.*, 2006). Together with the stress fibers and other cytoskeletal elements, they play important

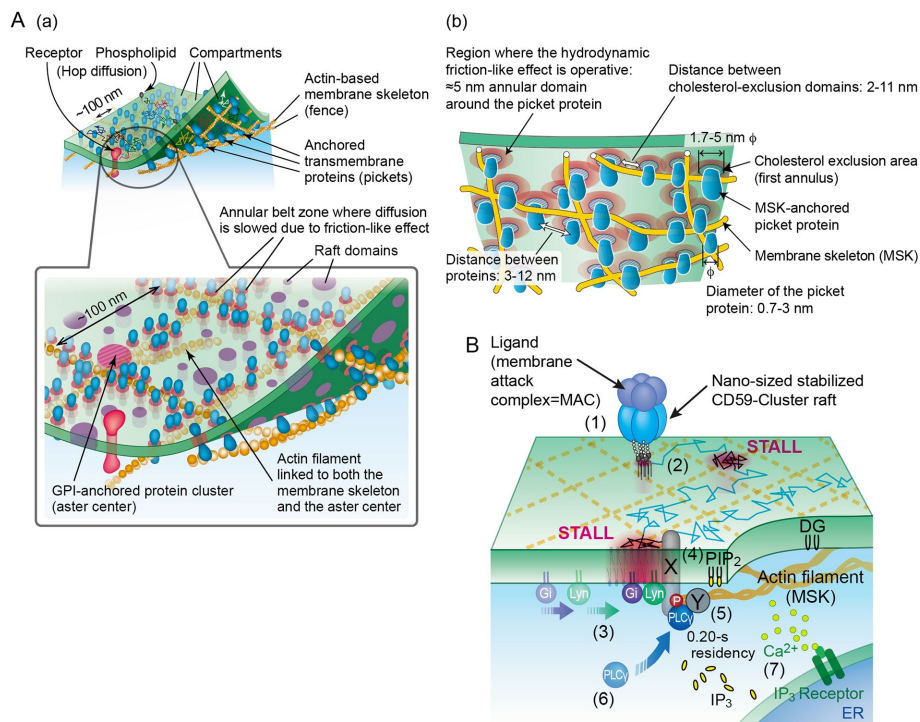


FIGURE 2: Actin-induced PM compartmentalization and its coupling with raft domains for signal transduction of GPI-AP receptors. (A) (a) Schematic model showing the actin-induced PM compartmentalization and the raft domains coexisting in the PM. Virtually the entire PM is compartmentalized by the actin-based membrane-skeleton meshes (fences) and rows of TM-protein pickets anchored to and aligned along the actin fence (blue molecules), with sizes between 40 and 230 nm (for different cell types). Both TM proteins (magenta) and lipids (black) undergo short-term confined diffusion within a compartment plus occasional hop movements to an adjacent compartment, termed hop diffusion. The phospholipids located in the PM outer leaflet also undergo hop diffusion due to the steric hindrance of TM picket proteins and the presence of the annular belt zone around the picket proteins, where the diffusion of membrane molecules is slowed due to the hydrodynamic friction-like effect of immobile picket proteins in the viscous liquid (red circular area surrounding blue TM picket proteins in the bottom figure; also see b). Raft domains would mostly be confined within the compartment (purple domains; see b for the mechanism). Meanwhile, submicronscale hetero GPI-AP complex rafts (pink with red slashes in the bottom figure) might interact with the actin membrane skeleton mesh and actin filaments associated with the membrane skeleton mesh, perhaps forming asters. The organization of the actin-based membrane skeleton dynamically changes, thus varying the compartment shapes all the time, partly due to myosin activities. (b) Proposed mechanisms showing how the rows of TM picket proteins anchored to and aligned along the actin-based membrane skeleton (fence) contribute to the formation of compartment boundaries and suppress the growth of raft domains across the compartment boundaries. For the diffusion of all PM-associated molecules, the TM picket proteins generate steric hindrance effects and, more importantly, the hydrodynamic friction-like effects of immobile molecules in the viscous liquid, which are propagated around two diameters of the immobilized TM domain cross-section, by approximately 0.7–3 nm (propagating 1.4–6 nm away from the TM picket protein surface; magenta gradation surrounding blue TM picket proteins). Monte Carlo simulations revealed that when ~20% of the compartment boundary is occupied by the TM picket proteins, the experimentally observed temporary confinement of phospholipids was observed (Fujiwara *et al.*, 2002). This is consistent with the presence of TM picket proteins 3–12 nm away from each other. The large variations in these numbers are due to the different sizes of the TM picket proteins. Raft growth across the compartment boundaries would be suppressed, because the compartment boundaries are full of CHOL-excluding zones formed by the first annular lipids or boundary lipids around the TM picket protein (Figure 1Bb-ii), with a belt thickness of ~0.5 nm (the areas shown by blue diagonal lines surrounding the blue TM picket proteins). Together with the steric hindrance effect of the TM picket proteins, they form CHOL-excluding zones of 1.7–5 nm in diameter (surrounding the TM picket proteins) located 2–11 nm away from each other. Therefore, for the growth of raft domains across the compartment boundaries, they might initially have to use these small gaps between the CHOL-excluding zones. (B) Schematic figure showing the process of raft-based signaling, using the case of CD59, a GPI-AP, as an example. See the main text for details.

roles in morphological changes and maintenance of the cell shape (which is the cell's PM shape), motility, endocytosis, and exocytosis. Among the cortical actin filaments, those closely apposed or bound to the PM cytoplasmic surface crisscross throughout this surface, forming a mesh-like structure, and thus are called the "actin membrane skeleton" (Bennett, 1990; Morone *et al.*, 2006, 2008). The actin membrane skeleton, which in some cases includes general cortical actin filaments, is a key constituent of the PM. Owing to its prevalence on the PM and ubiquity among cells, we will advance the actin-centered view of the PM here, in addition to the CHOL-centered view.

The entire bulk PM is compartmentalized (~100 nm and in the range of 30–230 nm, depending on the cell line) by the actin-based membrane-skeleton "fences" and rows of TM-protein "pickets" anchored to and aligned along these fences (Figure 2Aa) (Fujiwara *et al.*, 2002, 2016; Murase *et al.*, 2004; Trimble and Grinstein, 2015; Ostrowski *et al.*, 2016; Freeman *et al.*, 2018). In the compartmentalized PM, both TM proteins and lipids undergo short-term confined diffusion within a compartment plus occasional hop movements to an adjacent compartment, which is termed hop diffusion (Figure 2Aa) (Fujiwara *et al.*, 2002, 2016, 2021a,b; Murase *et al.*, 2004; Kusumi *et al.*, 2005, 2012a,b; Jaqaman and Grinstein, 2012; Xia *et al.*, 2019). As a consequence, each molecule in the PM exhibits two diffusion coefficients: the microscopic diffusion coefficient (D_{micro} : 3–10 $\mu\text{m}^2/\text{s}$), describing the unhindered diffusion within a compartment, and the macroscopic diffusion coefficient (D_{MACRO} : 0.1–1 $\mu\text{m}^2/\text{s}$), determined by the compartment size and the hop frequency across intercompartmental boundaries composed of the picket fence.

The TM picket proteins would not have to be packed on the actin filament meshes (Fujiwara *et al.*, 2002). Owing to the hydrodynamic friction-like effect of immobile molecules in viscous liquid, the diffusion coefficients of molecules within ~5 nm from the TM picket proteins would be greatly decreased (Figure 2Ab). Therefore, ~20% picket coverage of the fence area would be sufficient to generate the diffusion barriers.

Only several microseconds are needed for a membrane molecule to pass the compartment boundary on an actin filament (assuming 5 $\mu\text{m}^2/\text{s}$ for the phospholipid diffusion coefficient within the compartment and 10 nm for the width of the compartment boundary). Therefore, if a TM protein binds to an actin filament for >10 μs , it would block the passage of membrane molecules

across the compartment boundary. Consequently, although the TM protein pickets might be dynamically exchanging with diffusing molecules all the time, the TM proteins transiently bound to an actin filament still work well as diffusion obstacles and creators of annular areas within which diffusion is slowed.

Membrane molecules probably move from one compartment to an adjacent one due to the temporary breakdown of the fence or pickets. Short-term severing and spatial fluctuations of the actin filament mesh, as well as temporary loss of the TM picket proteins, would provide space for the passage of membrane molecules. For example, in the erythrocyte membrane, by pulling the spectrin meshwork with laser tweezers, Tomishige *et al.* (1998) found that spectrin tetramer dissociation to dimers (severing of the fence) is a key step for the hop movement of band 3, a TM protein (spectrin tetramer-dimer equilibrium [SPEQ] gate model) (Tsuiji *et al.*, 1988; Bennett, 1990; Tomishige *et al.*, 1998). Therefore, it is wrong to assume that such picket fences are static structures, as mentioned by some authors (Gowrishankar *et al.*, 2012; Freeman *et al.*, 2018). In longer timescales, laser tweezer experiments in which membrane molecules were laterally dragged in the PM plane revealed that the compartment boundaries shift and break within a minute (Ritchie and Kusumi, 2002).

Actin membrane skeleton is dynamically reorganized and continually modified by ATP- and myosin II-dependent processes

The hop movements of membrane molecules and the laser tweezer data suggest temporary severing and spatial fluctuations of the actin filament mesh, as well as dynamic large-scale modifications of the actin membrane skeleton. Superresolution microscopy of cortical actin filaments labeled with Lifeact-mGFP in live cells, conducted at time resolutions of 0.5–2.3 s and spatial resolutions of ~120 nm, detected actin clusters linking two or more actin filaments in the fine actin meshwork (confirmed by phalloidin staining using fixed cells), acting as nodes of the meshwork (Shirai *et al.*, 2017). About two-thirds of the actin nodes are located within 3.5 nm from the PM cytoplasmic surface, as found by using Lifeact linked to a TM peptide (Lifeact-TM), indicating that the majority of the observed actin nodes are on the actin membrane skeleton (Shirai *et al.*, 2017). Interestingly, the use of Lifeact-TM revealed that 89% of the stress fibers are also in the proximity (within 3.5 nm) of the PM cytoplasmic surface. The node formation depended on the Arp2/3 actin nucleation and filament branching activities.

The actin nodes dynamically moved on/along the actin meshwork in a myosin II-dependent manner. However, despite these myosin II-dependent movements of the actin nodes in the actin membrane skeleton, myosin II is not present in the actin nodes. Myosin II is probably located near the nodes, because it induces their directed and jittering diffusion-like movements. The fluctuating movements of the actin node are caused by several nearby myosin II filaments, which undergo a tug of war over the actin node.

These ATP-dependent active processes might be involved in the formation and dynamics of the actin membrane skeleton meshwork. As described, scanning optical trap experiments demonstrated that the PM compartments drift and change shapes in less than a minute (Ritchie and Kusumi, 2002).

INTERACTION OF THE ACTIN-BASED MEMBRANE SKELETON AND CORTICAL ACTIN FILAMENTS WITH RAFT DOMAINS

In this section, we describe the relationship between CHOL-centered raft domains and the actin-based membrane skeleton.

Raft exclusion from PM compartment boundaries by rows of TM picket proteins aligned along the actin membrane skeleton fence

In general, TM proteins and CHOL are sterically nonconformable with each other, due to the rigid α -helical structure and the rugged surface (due to the amino acid side chains protruding from the α -helix) of the TM domain and the rigid, bulky tetracyclic CHOL structure (Figure 1Bb) (however, see the paragraph after the next one). Therefore, raft domains, whether they exist in only the PM outer leaflet or in both the outer and inner leaflets, would hardly grow across the compartment boundaries where the TM picket proteins are abundant. Consequently, the sizes of raft domains in the PM would be limited by the meshes of the actin membrane skeleton. This conclusion is supported by *in vitro* experiments in which actin was placed on the supported bilayer or GUVs and by simulations (Honigmann *et al.*, 2014; Arumugam *et al.*, 2015).

In addition, the GPMV experiments revealed that cooling-induced large micronscale phase separation into Lo-phase-like and Ld-phase-like domains can occur only after the removal of the actin membrane skeleton (Baumgart *et al.*, 2007; Lingwood *et al.*, 2008; Levental *et al.*, 2009, 2010; Johnson *et al.*, 2010). These results clearly showed that the actin membrane skeleton blocks the formation of micronscale raft domains.

Meanwhile, some TM proteins have been proposed to partition into raft domains (Levental *et al.*, 2010). Furthermore, immune TM receptors reportedly take advantage of raft domains in their signaling. These results are summarized in *Detailed explanation 5*, which is placed right before *Concluding remarks*.

We sometimes hear arguments about whether the PM is organized by actin-based compartmentalization or raft domains, but it is important to realize that both occur, as clarified by the preceding discussions; also see Kusumi *et al.* (2012a,b). The actin membrane skeleton compartmentalizes the entire PM, and the nanoscale (2–200 nm) rafts exist within the compartments (Figure 2A).

Because both actin-induced compartments and raft domains coexist in the PM and the sizes and densities of raft domains as well as the sizes of the actin-induced compartments vary greatly among different types of cells, applications of the so-called diffusion law for interpreting the results of fluorescence correlation spectroscopy obtained by confocal and stimulated emission depletion (STED) microscopy must be done carefully. Depending on the details of the raft domains and actin-induced compartments, the dependence of the diffusion coefficients on the observation area size would vary in very complex ways (Wawrezynieck *et al.*, 2005; Andrade *et al.*, 2015; Schneider *et al.*, 2017; Veerapathiran and Wohland, 2018; Sezgin *et al.*, 2019).

Submicronscales–micronscales rafts containing heteromixtures of GPI-APs are coupled with cytoplasmic actin filaments by way of TM proteins and long, saturated phosphatidylserine bound to actin filaments

As described, Mayor's group found submicronscales–micronscales rafts containing heteromixtures of GPI-APs in the PM outer leaflet, whose formation is actively driven by actomyosin, located on the PM inner surface. These submicronscales–micronscales rafts are considered to be surrounded by radially spreading actin filaments. Such structures are termed "asters," and were visualized *in vitro* (Gowrishankar *et al.*, 2012) but apparently not *in vivo*. The asters are colocalized with myosin II and filamin. For beautiful and clear presentations of asters and the actin meshwork on the PM, see Figure 1b of Honigmann and Pralle (2016).

How can these actin filaments located on the PM inner surface become coupled to the hetero-GPI-AP complex rafts in the PM outer leaflet? Mayor's group proposed that clusters of phosphatidylserine (PS), with long, saturated acyl chains located in the inner leaflet, are bound to actin filaments and also coupled to the sub-micron-scale–micron-scale rafts containing heteromixtures of GPI-APs in the outer leaflet by interdigitation in the middle of the bilayer (Raghupathy *et al.*, 2015). Because CHOL is much shorter than the long, saturated chains of GPI-APs and PS (Figure 1Ba), the inner surfaces of both the PS and GPI-AP clusters in the central part of the bilayer are rough, and thus once they come together, they might not readily break apart from each other. The transbilayer coupling is enhanced upon the activation of $\beta 1$ integrin, which triggers actin nucleation via formins and myosin, and the involvement of talin and the mechanotransducer vinculin in the cluster (Kalappurakkal *et al.*, 2019). Interestingly, GPI-AP clustering was required for integrin-induced cell spreading and migration.

Some of the actin nodes detected by superresolution microscopy might be the same as actin asters, but some may differ because myosin II and filamin A are not appreciably colocalized with the actin nodes (Shirai *et al.*, 2017). Previously, such actin clusters (nodes and asters) were found in vitro (Köster *et al.*, 2016) or after drug-induced partial actin depolymerization in live cells (Luo *et al.*, 2013). However, superresolution microscopy of live cells clarified that actin nodes constitutively exist in the actin membrane skeleton within 3.5 nm from the PM inner surface and are dynamically driven by myosin II in an ATP-dependent manner (Shirai *et al.*, 2017).

Involvement of actin membrane skeleton in GPI-AP receptors' raft-based signaling

Reports about the involvement of the actin membrane skeleton (or cortical actin filaments) in the signal transduction of GPI-AP receptors have been quite scarce. Here, we summarize the results reported previously (Suzuki *et al.*, 2007a,b), which are rare publications addressing this issue. When CD59, a GPI-AP working as the receptor for the membrane attack complex, is engaged, it forms clusters containing an average of four to five CD59 molecules, which in turn form nano-sized stabilized CD59-cluster rafts (Figure 2B1). Experimentally, this process could be mimicked by closely cross-linking the CD59 molecules by the addition of 40-nm gold particles coated with an anti-CD59 monoclonal antibody. Both the natural ligation and artificial cross-linking can trigger very similar intracellular signals, such as PLC γ recruitment to CD59-cluster rafts, leading to IP $_3$ production and then to intracellular calcium responses (Figure 2B).

Engaged CD59-cluster rafts exhibited very peculiar behaviors. They repeatedly and continually undergo temporary immobilizations lasting for 0.56 s (exponential lifetime) that are induced by the binding of CD59-cluster rafts to the actin-based membrane skeleton (called stimulation-induced arrest of lateral diffusion = STALL; Figure 2B2). This binding is induced by Src-family kinases, such as Lyn, which is activated by G α_i , the alpha subunit of the inhibitory trimeric G protein, after they are both recruited to CD59-cluster rafts (Figure 2B3). The protein(s) phosphorylated by Lyn is unknown, but it (or one of them) could be an as-yet-unknown TM protein X, which might mediate the PLC γ recruitment to the site on the PM inner surface linked to the CD59-cluster raft located in the PM outer leaflet (Figure 2B4). Meanwhile, a cytoplasmic protein Y might also be involved in this process (Figure 2B5).

Very interestingly, PLC γ is recruited to the CD59-cluster only when the CD59-cluster raft is undergoing temporary immobilization due to its binding to the actin-based membrane skeleton (Figure 2B6). These results suggest the possibility that signal transduction

platforms for GPI-APs might abundantly exist on the actin-based membrane skeleton. When the CD59-cluster raft meets G α_i and Lyn on the platform, it becomes temporarily immobilized on the signaling platform by binding to proteins X and Y, which are in turn phosphorylated by Lyn, producing the binding sites for PLC γ . PLC γ recruited to CD59-cluster rafts produces IP $_3$ and diacylglycerol, leading to intracellular Ca $^{2+}$ mobilization and PKC activation (Figure 2B7).

Detailed explanation 5: TM proteins partitioning into raft domains and TM receptors taking advantage of raft domains for their signaling

Note that some TM proteins have been proposed to partition into raft domains (Levental *et al.*, 2010). Lorent *et al.* (2017) identified three physical features of the TM domains that independently affect the raft partitioning of TM proteins: smaller surface area, longer TM domain, and palmitoylation. More specifically, they represent smaller protruding amino acid side chains from the α -helical TM domain, matching of the hydrophobic length of the TM domain with the extended saturated acyl chains (due to the association with CHOL), and smoothing of the rugged TM domain surface by the palmitoyl chains, respectively. These features might be coupled with the dimerization–oligomerization of TM proteins linked by palmitoyl chains. Rhodopsin, a G protein–coupled receptor with seven TM domains, has two covalently linked palmitoyl chains, but becomes associated with raft domains only upon dimer formation (Seno and Hayashi, 2017; Hayashi *et al.*, 2019). This result suggests that the rugged parts of the TM domain surface of the dimer are more easily covered with four palmitate chains than those of the monomer with two palmitate chains.

Immune receptors, including high-affinity Fc ϵ receptors (Fc ϵ RI) in mast cells and B-cell receptors, take advantage of the raft domains that the ligand-induced receptor oligomers generate in/around them to enhance their downstream signaling. The involvement of raft domains in immune receptor signaling had long been suspected, but it was difficult to show unequivocally. However, this difficulty was solved by developing/improving microscopic imaging-analysis methods.

By improving imaging fluorescence correlation spectroscopy, Baird and colleagues revealed that stabilized Lo-like nanoscale raft domains are created around clustered Fc ϵ RI in immune mast cells (Bag *et al.*, 2021). These domains strongly augment the Lyn recruitment and suppress the recruitment of the TM phosphatase PTP α . Proof of the Lyn recruitment to clustered Fc ϵ RI had previously been elusive, but extensive examinations of very many molecular trajectories (several tens of thousands), made possible by the improvement and application of imaging fluorescence correlation spectroscopy, unequivocally revealed Lyn recruitment to clustered Fc ϵ RI. This result is consistent with the enhanced recruitment of sphingomyelin, a prototypical raftophilic phospholipid, to antigen-induced clusters of Fc ϵ RI but not to Fc ϵ RI in resting cells, found by single-molecule imaging tracking of a newly developed fluorescently labeled sphingomyelin (Kinoshita *et al.*, 2017).

In immune B cells, by applying a pair cross-correlation analysis method to superresolution single-molecule localization microscopy data (Stone and Veatch, 2014), Veatch and colleagues demonstrated that stimulation-induced B-cell receptor (BCR) clusters induce Lo-phase-like domains around them, which are capable of sorting key regulators of BCR activation (Stone *et al.*, 2017).

Taken together, these results provide evidence for the role of the receptor clustering–induced membrane domains and a plausible mechanism for recruiting downstream signaling molecules to the receptor clusters. They agree well with the signaling raft domain

formation induced by the clustering of a GPI-AP, CD59 (Suzuki *et al.*, 2007a,b, 2012) and suggest that similar mechanisms are employed in many other receptor signaling pathways (Kusumi *et al.*, 2004; Koyama-Honda *et al.*, 2020).

For other examples in which raft-based interactions might be involved in the signal transduction by TM receptors, refer to the following papers: Sohn *et al.* (2008); Coskun *et al.* (2011); Chung *et al.* (2016); Shelby *et al.* (2016).

CONCLUDING REMARKS

We propose two major updates of the Singer–Nicolson fluid mosaic model. One is the CHOL-induced cooperativity-based assembly of CHOL and molecules containing saturated acyl chains, which represents the transition of the fluid mosaic model from a simple liquid model to a model of the liquid containing various metastable liquid-like clusters of 2–20 nm in diameter, called raft domains. The formation of such lower-nanoscale liquid rafts is enhanced by homophilic protein–protein interactions in the case of GPI-APs, leading to the formation of GPI-AP homodimer rafts, which are one of the basic unit rafts involved in building greater raft domains containing GPI-APs. Upon extracellular stimulation, GPI-AP receptors form ligand-induced clusters, which induce greater and stabilized raft domains with the help of raft-lipid interactions, and these enlarged, stabilized raft domains become responsible for the downstream signaling. Note that the cooperativity for the raft domain formation is due not only to the accommodating interactions between CHOL and saturated acyl chains, but also to the nonconformable interactions between CHOL and unsaturated acyl chains + proteins' TM domains.

The other update is the compartmentalization of the entire PM by the actin-based membrane skeleton (fence), as well as TM proteins anchored to and aligned along the membrane skeleton (pickets). This compartmentalization occurs throughout the entire PM with compartment sizes between 30 and 230 nm, which depends on the cell type. However, within each compartment, the fluid mosaic model with the upgrade of the presence of many nanoscale liquid raft domains is perfectly correct.

Raft domains are excluded from the picket-fence compartmental boundary areas due to their nonconformability with the TM pickets. Therefore, the raft domains tend to be localized within a compartment and thus their sizes are smaller than the compartment sizes. However, the stabilized raft domains induced by the engaged GPI-AP receptors might be able to indirectly associate with the actin-based membrane skeleton by way of the signal transduction platform bound to the actin-based membrane skeleton. This was deduced by the finding that the stabilized raft domains induced by the engaged GPI-AP receptor clusters undergo actin-dependent temporary immobilizations and signal transduction during immobilization.

In this review, we have advanced the argument that the CHOL and actin-centered views of the PM provide excellent perspectives for understanding PM structure, molecular dynamics, and functions, while coping with the VUCA of the PM. We hope that readers have been convinced of the usefulness of these views and that they will start considering the PM accordingly.

ACKNOWLEDGMENTS

This work was supported in part by Grants-in-Aid for Scientific Research from the Japan Society for the Promotion of Science (JSPS) (Wakate to T.A.T. [21K15058], Kiban B to T.K.F. [16H04775, 20H02585], Kiban B to K.G.N.S. [18H02401, 21H02424], and Kiban S and A to A.K. [16H06386 and 21H04772, respectively]), Grants-in-Aid for Challenging Research (Exploratory) from JSPS to T.K.F.

(18K19001) and to A.K. (22K19334), Grants-in-Aid from the Ministry of Education, Culture, Sports, Science and Technology of Japan (MEXT) for Transformative Research Areas (A) to T.K.F. (21H05252) and for Innovative Areas to K.G.N.S. (18H04671), a Japan Science and Technology Agency (JST) grant in the program of the Core Research for Evolutional Science and Technology (CREST) in the field of “Biodynamics” to A.K. and that in the field of “Extracellular Fine Particles” to K.G.N.S. (JPMJCR18H2), a JST grant in the program of “Development of Advanced Measurements and Analysis Systems” to A.K. and T.K.F., JST grant ACT-X to T.A.T. (JPMJAX211B), and a grant from the Takeda Foundation to K.G.N.S. WPI-iCeMS of Kyoto University is supported by the World Premiere Research Center Initiative (WPI) of MEXT. We thank the current and past colleagues of our laboratories for their critical discussions with us and help in formulating this review. We also thank the editor and two editorial board members who critically reviewed this article and provided constructive and important suggestions, which greatly helped us to improve this perspective article. A.K. lost two mentors in a row recently. His PhD advisor, Prof. Shun-ichi Ohnishi of Kyoto University, who is responsible for A.K.'s biophysics and biochemistry, passed away in 2021, and his postdoc advisor, Prof. James S. Hyde of the Medical College of Wisconsin, who is responsible for A.K.'s physics and biophysics, passed away in 2022. A.K.'s second postdoc advisor, Prof. Malcolm S. Steinberg of Princeton University, who is responsible for A.K.'s cellular and developmental biology, passed away some time ago (2012). Other authors of this article are like their grandchildren. Therefore, we dedicate this article to Ohnishi-sensei, Jim, and Mal.

REFERENCES

- Abrami L, Liu S, Cosson P, Leppla SH, van der Goot FG (2003). Anthrax toxin triggers endocytosis of its receptor via a lipid raft-mediated clathrin-dependent process. *J Cell Biol* 160, 321–328.
- Abrams ME, Johnson KA, Perelman SS, Zhang L, Endapally S, Mar KB, Thompson BM, McDonald JG, Schoggins JW, Radhakrishnan A, *et al.* (2020). Oxysterols provide innate immunity to bacterial infection by mobilizing cell surface accessible cholesterol. *Nat Microbiol* 5, 929–942.
- Andrade DM, Clausen MP, Keller J, Mueller V, Wu C, Bear JE, Hell SW, Lagerholm BC, Eggeling C (2015). Cortical actin networks induce spatiotemporal confinement of phospholipids in the plasma membrane—a minimally invasive investigation by STED-FCS. *Sci Rep* 5, 11454.
- Arnold AM, Schneider MC, Hüsön C, Sablatnig R, Brameshuber M, Baumgart F, Schütz GJ (2020). Verifying molecular clusters by 2-color localization microscopy and significance testing. *Sci Rep* 10, 4230.
- Arumugam S, Schmieder S, Pezeshkian W, Becken U, Wunder C, Chinnappan D, Ipsen JH, Kenworthy AK, Lencer W, Mayor S, *et al.* (2021). Ceramide structure dictates glycosphingolipid nanodomain assembly and function. *Nat Commun* 12, 3675.
- Arumugam S, Petrov EP, Schwille P (2015). Cytoskeletal pinning controls phase separation in multicomponent lipid membranes. *Biophys J* 108, 1104–1113.
- Bag N, Wagenknecht-Wiesner A, Lee A, Shi SM, Holowka DA, Baird BA (2021). Lipid-based and protein-based interactions synergize transmembrane signaling stimulated by antigen clustering of IgE receptors. *Proc Natl Acad Sci USA* 118, e2026583118.
- Baumgart T, Hammond AT, Sengupta P, Hess ST, Holowka DA, Baird BA, Webb WW (2007). Large-scale fluid/fluid phase separation of proteins and lipids in giant plasma membrane vesicles. *Proc Natl Acad Sci USA* 104, 3165–3170.
- Bennett V (1990). Spectrin-based membrane skeleton: a multipotential adaptor between plasma membrane and cytoplasm. *Physiol Rev* 70, 1029–1065.
- Bennis WG, Nanus B (1986). *Leaders: The Strategies for Taking Charge*, New York, NY: Harper & Row.
- Bhatia T, Cornelius F, Ipsen JH (2016). Exploring the raft-hypothesis by probing planar bilayer patches of free-standing giant vesicles at nanoscale resolution, with and without Na,K-ATPase. *Biochim Biophys Acta* 1858, 3041–3049.

- Bhatia T, Husen P, Ipsen JH, Bagatolli LA, Simonsen AC (2014). Fluid domain patterns in free-standing membranes captured on a solid support. *Biochim Biophys Acta* 1838, 2503–2510.
- Bourdeau RW, Malito E, Chenal A, Bishop BL, Musch MW, Villereal ML, Chang EB, Mosser EM, Rest RF, Tang W-J (2009). Cellular functions and X-ray structure of anthrolysin O, a cholesterol-dependent cytolyisin secreted by *Bacillus anthracis*. *J Biol Chem* 284, 14645–14656.
- Brown DA, Rose JK (1992). Sorting of GPI-anchored proteins to glycolipid-enriched membrane subdomains during transport to the apical cell surface. *Cell* 68, 533–544.
- Cho W, Ralko A, Sharma A (2022). An in situ fluorescence assay for cholesterol transporter activity of the patched. *Methods Mol Biol* 2374, 37–47.
- Chung I, Reichelt M, Shao L, Akita RW, Koeppen H, Rangell L, Schaefer G, Mellman I, Sliwkowski MX (2016). High cell-surface density of HER2 deforms cell membranes. *Nat Commun* 7, 12742.
- Cornell CE, Mileant A, Thakkar N, Lee KK, Keller SL (2020). Direct imaging of liquid domains in membranes by cryo-electron tomography. *Proc Natl Acad Sci USA* 117, 19713–19719.
- Coskun Ü, Grzybek M, Drechsel D, Simons K (2011). Regulation of human EGF receptor by lipids. *Proc Natl Acad Sci USA* 108, 9044–9048.
- Courtney KC, Fung KY, Maxfield FR, Fairm GD, Zha X (2018). Comment on “Orthogonal lipid sensors identify transbilayer asymmetry of plasma membrane cholesterol.” *eLife* 7, e38493.
- Das A, Brown MS, Anderson DD, Goldstein JL, Radhakrishnan A (2014). Three pools of plasma membrane cholesterol and their relation to cholesterol homeostasis. *eLife* 3, e02882.
- Dotti CG, Parton RG, Simons K (1991). Polarized sorting of glypiated proteins in hippocampal neurons. *Nature* 349, 158–161.
- Eisenberg S, Beckett AJ, Prior IA, Dekker FJ, Hedberg C, Waldmann H, Ehrlich M, Henis YI (2011). Raft protein clustering alters N-Ras membrane interactions and activation pattern. *Mol Cell Biol* 31, 3938–3952.
- Endapally S, Frias D, Grzemska M, Gay A, Tomchick DR, Radhakrishnan A (2019). Molecular discrimination between two conformations of sphingomyelin in plasma membranes. *Cell* 176, 1040–1053.e17.
- Farrand AJ, LaChapelle S, Hotze EM, Johnson AE, Tweten RK (2010). Only two amino acids are essential for cytolytic toxin recognition of cholesterol at the membrane surface. *Proc Natl Acad Sci USA* 107, 4341–4346.
- Fessler MB, Parks JS (2011). Intracellular lipid flux and membrane microdomains as organizing principles in inflammatory cell signaling. *J Immunol* 187, 1529–1535.
- Fiedler K, Kobayashi T, Kurzchalia TV, Simons K (1993). Glycosphingolipid-enriched, detergent-insoluble complexes in protein sorting in epithelial cells. *Biochemistry* 32, 6365–6373.
- Freeman SA, Vega A, Riedl M, Collins RF, Ostrowski PP, Woods EC, Bertozzi CR, Tammi MI, Lidke DS, Johnson P, et al. (2018). Transmembrane pickets connect cyto- and pericellular skeletons forming barriers to receptor engagement. *Cell* 172, 305–317.e10.
- Fujiwara T, Ritchie K, Murakoshi H, Jacobson K, Kusumi A (2002). Phospholipids undergo hop diffusion in compartmentalized cell membrane. *J Cell Biol* 157, 1071–1082.
- Fujiwara TK, Iwasawa K, Kalay Z, Tsunoyama TA, Watanabe Y, Umemura YM, Murakoshi H, Suzuki KGN, Nemoto YL, Morone N, et al. (2016). Confined diffusion of transmembrane proteins and lipids induced by the same actin meshwork lining the plasma membrane. *Mol Biol Cell* 27, 1101–1119.
- Fujiwara TK, Takeuchi S, Kalay Z, Nagai Y, Tsunoyama TA, Kalkbrenner T, Chen LH, Shibata ACE, Iwasawa K, Ritchie KP, et al. (2021a). Focal adhesion membrane is dotted with protein islands and partitioned for molecular hop diffusion. *BioRxiv*, 2021.10.26.465868.
- Fujiwara TK, Takeuchi S, Kalay Z, Nagai Y, Tsunoyama TA, Kalkbrenner T, Iwasawa K, Ritchie KP, Suzuki KGN, Kusumi A (2021b). Development of ultrafast camera-based imaging of single fluorescent molecules and live-cell PALM. *BioRxiv*, 2021.10.26.465864.
- Goswami D, Gowrishankar K, Bilgrami S, Ghosh S, Raghupathy R, Chadda R, Vishwakarma R, Rao M, Mayor S (2008). Nanoclusters of GPI-anchored proteins are formed by cortical actin-driven activity. *Cell* 135, 1085–1097.
- Gowrishankar K, Ghosh S, Saha S, Rumamol C, Mayor S, Rao M (2012). Active remodeling of cortical actin regulates spatiotemporal organization of cell surface molecules. *Cell* 149, 1353–1367.
- Green JM, Zheleznyak A, Chung J, Lindberg FP, Sarfati M, Frazier WA, Brown EJ (1999). Role of cholesterol in formation and function of a signaling complex involving $\alpha\text{v}\beta 3$, integrin-associated protein (Cd47), and heterotrimeric G proteins. *J Cell Biol* 146, 673–682.
- Harder T, Simons K (1997). Caveolae, DIGs, and the dynamics of sphingolipid-cholesterol microdomains. *Curr Opin Cell Biol* 9, 534–542.
- Hayashi F, Saito N, Tanimoto Y, Okada K, Morigaki K, Seno K, Maekawa S (2019). Raftophilic rhodopsin-clusters offer stochastic platforms for G protein signalling in retinal discs. *Commun Biol* 2, 209.
- Heberle FA, Doktorova M, Scott HL, Skinkle AD, Waxham MN, Levental I (2020). Direct label-free imaging of nanodomains in biomimetic and biological membranes by cryogenic electron microscopy. *Proc Natl Acad Sci USA* 117, 19943–19952.
- Heberle FA, Petruzielo RS, Pan J, Drazba P, Kuc erka N, Standaert RF, Feigenson GW, Katsaras J (2013). Bilayer thickness mismatch controls domain size in model membranes. *J Am Chem Soc* 135, 6853–6859.
- Heberle FA, Wu J, Goh SL, Petruzielo RS, Feigenson GW (2010). Comparison of three ternary lipid bilayer mixtures: FRET and ESR reveal nanodomains. *Biophys J* 99, 3309–3318.
- Holthuis JCM, Menon AK (2014). Lipid landscapes and pipelines in membrane homeostasis. *Nature* 510, 48–57.
- Honerkamp-Smith AR, Cicuta P, Collins MD, Veatch SL, den Nijs M, Schick M, Keller SL (2008). Line tensions, correlation lengths, and critical exponents in lipid membranes near critical points. *Biophys J* 95, 236–246.
- Honigmann A, Pralle A (2016). Compartmentalization of the cell membrane. *J Mol Biol* 428, 4739–4748.
- Honigmann A, Sadeghi S, Jan K, Hell SW, Eggeling C, Vink R (2014). A lipid bound actin meshwork organizes liquid phase separation in model membranes. *Biophys J* 106, 634a.
- Hunter I, Nixon GF (2006). Spatial compartmentalization of tumor necrosis factor (TNF) receptor 1-dependent signaling pathways in human airway smooth muscle cells. *J Biol Chem* 281, 34705–34715.
- Jacobson K, Liu P, Lagerholm BC (2019). The lateral organization and mobility of plasma membrane components. *Cell* 177, 806–819.
- Jaqaman K, Grinstein S (2012). Regulation from within: the cytoskeleton in transmembrane signaling. *Trends Cell Biol* 22, 515–526.
- Johnson BB, Moe PC, Wang D, Rossi K, Trigatti BL, Heuck AP (2012). Modifications in perflingolysin O domain 4 alter the cholesterol concentration threshold required for binding. *Biochemistry* 51, 3373–3382.
- Johnson SA, Stinson BM, Go MS, Carmona LM, Reminick JI, Fang X, Baumgart T (2010). Temperature-dependent phase behavior and protein partitioning in giant plasma membrane vesicles. *Biochim Biophys Acta* 1798, 1427–1435.
- Kalappurakkal JM, Anilkumar AA, Patra C, van Zanten TS, Sheetz MP, Mayor S (2019). Integrin mechano-chemical signaling generates plasma membrane nanodomains that promote cell spreading. *Cell* 177, 1738–1756.e23.
- Kalappurakkal JM, Sil P, Mayor S (2020). Toward a new picture of the living plasma membrane. *Protein Sci* 29, 1355–1365.
- Kenworthy AK, Nichols BJ, Remmert CL, Hendrix GM, Kumar M, Zimmerberg J, Lippincott-Schwartz J (2004). Dynamics of putative raft-associated proteins at the cell surface. *J Cell Biol* 165, 735–746.
- Kinnebrew M, Iverson EJ, Patel BB, Pusapati GV, Kong JH, Johnson KA, Luchetti G, Eckert KM, McDonald JG, Covey DF, et al. (2019). Cholesterol accessibility at the ciliary membrane controls hedgehog signaling. *eLife* 8, e50051.
- Kinoshita M, Suzuki KGN, Matsumori N, Takada M, Ano H, Morigaki K, Abe M, Makino A, Kobayashi T, Hirokawa KM, et al. (2017). Raft-based sphingomyelin interactions revealed by new fluorescent sphingomyelin analogs. *J Cell Biol* 216, 1183–1204.
- Kinoshita T, Fujita M (2015). Biosynthesis of GPI-anchored proteins: special emphasis on GPI lipid remodeling. *J Lipid Res* 57, 6–24.
- Komura N, Suzuki KGN, Ando H, Konishi M, Koikeda M, Imamura A, Chadda R, Fujiwara TK, Tsuboi H, Sheng R, et al. (2016). Raft-based interactions of gangliosides with a GPI-anchored receptor. *Nat Chem Biol* 12, 402–410.
- Korinek M, Vyklicky V, Borovska J, Lichnerova K, Kaniakova M, Krausova B, Krusek J, Balik A, Smejkalova T, Horak M, et al. (2015). Cholesterol modulates open probability and desensitization of NMDA receptors. *J Physiol* 593, 2279–2293.
- Köster DV, Husain K, Iljazi E, Bhat A, Bieling P, Mullins RD, Rao M, Mayor S (2016). Actomyosin dynamics drive local membrane component organization in an in vitro active composite layer. *Proc Natl Acad Sci USA* 113, E1645–E1654.
- Koyama-Honda I, Fujiwara TK, Kasai RS, Suzuki KGN, Kajikawa E, Tsuboi H, Tsunoyama TA, Kusumi A (2020). High-speed single-molecule imaging reveals signal transduction by induced transbilayer raft phases. *J Cell Biol* 219, e202006125.
- Kusumi A, Fujiwara TK, Tsunoyama TA, Kasai RS, Liu A, Hirokawa KM, Kinoshita M, Matsumori N, Komura N, Ando H, et al. (2020). Defining raft domains in the plasma membrane. *Traffic* 21, 106–137.
- Kusumi A, Fujiwara TK, Chadda R, Xie M, Tsunoyama TA, Kalay Z, Kasai RS, Suzuki KGN (2012a). Dynamic organizing principles of the plasma

- membrane that regulate signal transduction: commemorating the fortieth anniversary of Singer and Nicolson's fluid-mosaic model. *Annu Rev Cell Dev Biol* 28, 215–250.
- Kusumi A, Fujiwara TK, Morone N, Yoshida KJ, Chadda R, Xie M, Kasai RS, Suzuki KGN (2012b). Membrane mechanisms for signal transduction: the coupling of the meso-scale raft domains to membrane-skeleton-induced compartments and dynamic protein complexes. *Semin Cell Dev Biol* 23, 126–144.
- Kusumi A, Koyama-Honda I, Suzuki K (2004). Molecular dynamics and interactions for creation of stimulation-induced stabilized rafts from small unstable steady-state rafts. *Traffic* 5, 213–230.
- Kusumi A, Nakada C, Ritchie K, Murase K, Suzuki K, Murakoshi H, Kasai RS, Kondo J, Fujiwara T (2005). Paradigm shift of the plasma membrane concept from the two-dimensional continuum fluid to the partitioned fluid: high-speed single-molecule tracking of membrane molecules. *Annu Rev Biophys Biomol Struct* 34, 351–378.
- Kusumi A, Tsunoyama TA, Hirose KM, Kasai RS, Fujiwara TK (2014). Tracking single molecules at work in living cells. *Nat Chem Biol* 10, 524–532.
- Kwik J, Boyle S, Fooksman D, Margolis L, Sheetz MP, Edidin M (2003). Membrane cholesterol, lateral mobility, and the phosphatidylinositol 4,5-bisphosphate-dependent organization of cell actin. *Proc Natl Acad Sci USA* 100, 13964–13969.
- Levental I, Byfield FJ, Chowdhury P, Gai F, Baumgart T, Janmey PA (2009). Cholesterol-dependent phase separation in cell-derived giant plasma-membrane vesicles. *Biochem J* 424, 163–167.
- Levental I, Levental KR, Heberle FA (2020). Lipid rafts: controversies resolved, mysteries remain. *Trends Cell Biol* 30, 341–353.
- Levental I, Lingwood D, Grzybek M, Coskun Ü, Simons K (2010). Palmitoylation regulates raft affinity for the majority of integral raft proteins. *Proc Natl Acad Sci USA* 107, 22050–22054.
- Lingwood D, Ries J, Schwille P, Simons K (2008). Plasma membranes are poised for activation of raft phase coalescence at physiological temperature. *Proc Natl Acad Sci USA* 105, 10005–10010.
- Lingwood D, Simons K (2010). Lipid rafts as a membrane-organizing principle. *Science* 327, 46–50.
- Liu S-L, Sheng R, Jung JH, Wang L, Stec E, O'Connor MJ, Song S, Bikkavilli RK, Winn RA, Lee D, et al. (2017). Orthogonal lipid sensors identify transbilayer asymmetry of plasma membrane cholesterol. *Nat Chem Biol* 13, 268–274.
- Lorent JH, Diaz-Rohrer B, Lin X, Spring K, Gorfe AA, Levental KR, Levental I (2017). Structural determinants and functional consequences of protein affinity for membrane rafts. *Nat Commun* 8, 1219.
- Luo W, Yu C, Lieu ZZ, Allard J, Mogilner A, Sheetz MP, Bershadsky AD (2013). Analysis of the local organization and dynamics of cellular actin networks. *J Cell Biol* 202, 1057–1073.
- Maekawa M, Fairn GD (2015). Complementary probes reveal that phosphatidylserine is required for the proper transbilayer distribution of cholesterol. *J Cell Sci* 128, 1422–1433.
- Makino A, Abe M, Ishitsuka R, Murate M, Kishimoto T, Sakai S, Hullin-Matsuda F, Shimada Y, Inaba T, Miyatake H, et al. (2017). A novel sphingomyelin/cholesterol domain-specific probe reveals the dynamics of the membrane domains during virus release and in Niemann-Pick type C. *FASEB J* 31, 1301–1322.
- Manley S, Gillette JM, Patterson GH, Shroff H, Hess HF, Betzig E, Lippincott-Schwartz J (2008). High-density mapping of single-molecule trajectories with photoactivated localization microscopy. *Nat Methods* 5, 155–157.
- Maxfield FR, Wüstner D (2012). Analysis of cholesterol trafficking with fluorescent probes. *Methods Cell Biol* 108, 367–393.
- McGraw KL, Fuhler GM, Johnson JO, Clark JA, Caceres GC, Sokol L, List AF (2012). Erythropoietin receptor signaling is membrane raft dependent. *PLoS One* 7, e34477.
- Monastyrskaya K, Hostettler A, Buergi S, Draeger A (2005). The NK1 receptor localizes to the plasma membrane microdomains, and its activation is dependent on lipid raft integrity. *J Biol Chem* 280, 7135–7146.
- Moran M, Miceli MC (1998). Engagement of GPI-linked CD48 contributes to TCR signals and cytoskeletal reorganization: a role for lipid rafts in T cell activation. *Immunity* 9, 787–796.
- Morone N, Fujiwara T, Murase K, Kasai RS, Ike H, Yuasa S, Usukura J, Kusumi A (2006). Three-dimensional reconstruction of the membrane skeleton at the plasma membrane interface by electron tomography. *J Cell Biol* 174, 851–862.
- Morone N, Nakada C, Umemura Y, Usukura J, Kusumi A (2008). Three-dimensional molecular architecture of the plasma-membrane-associated cytoskeleton as reconstructed by freeze-etch electron tomography. *Methods Cell Biol* 88, 207–236.
- Murase K, Fujiwara T, Umemura Y, Suzuki K, Iino R, Yamashita H, Saito M, Murakoshi H, Ritchie K, Kusumi A (2004). Ultrafine membrane compartments for molecular diffusion as revealed by single molecule techniques. *Biophys J* 86, 4075–4093.
- Nakamura M, Sekino N, Iwamoto M, Ohno-Iwashita Y (1995). Interaction of theta-toxin (perfringolysin O), a cholesterol-binding cytotoxin, with liposomal membranes: change in the aromatic side chains upon binding and insertion. *Biochemistry* 34, 6513–6520.
- Ohno-Iwashita Y, Iwamoto M, Ando S, Mitsui K, Iwashita S (1990). A modified theta-toxin produced by limited proteolysis and methylation: a probe for the functional study of membrane cholesterol. *Biochim Biophys Acta* 1023, 441–448.
- Omidvar N, Wang ECY, Brennan P, Longhi MP, Smith RAG, Morgan BP (2006). Expression of glycosylphosphatidylinositol-anchored CD59 on target cells enhances human NK cell-mediated cytotoxicity. *J Immunol* 176, 2915–2923.
- Ostrowski PP, Grinstein S, Freeman SA (2016). Diffusion barriers, mechanical forces, and the biophysics of phagocytosis. *Dev Cell* 38, 135–146.
- Ota K, Leonardi A, Mikelj M, Skočaj M, Wohlschlager T, Künzler M, Aebi M, Narat M, Križaj I, Anderluh G, et al. (2013). Membrane cholesterol and sphingomyelin, and streptolysin A are obligatory for pore-formation by a MACPF/CDC-like pore-forming protein, pleurotolysin B. *Biochimie* 95, 1855–1864.
- Owen DM, Williamson DJ, Magenau A, Gaus K (2012). Sub-resolution lipid domains exist in the plasma membrane and regulate protein diffusion and distribution. *Nat Commun* 3, 1256.
- Pageon SV, Nicovich PR, Mollazade M, Tabarin T, Gaus K (2016). Clus-DoC: a combined cluster detection and colocalization analysis for single-molecule localization microscopy data. *Mol Biol Cell* 27, 3627–3636.
- Pathak P, London E (2011). Measurement of lipid nanodomain (raft) formation and size in sphingomyelin/POPC/cholesterol vesicles shows TX-100 and transmembrane helices increase domain size by coalescing preexisting nanodomains but do not induce domain formation. *Biophys J* 101, 2417–2425.
- Paulick MG, Bertozzi CR (2008). The glycosylphosphatidylinositol anchor: a complex membrane-anchoring structure for proteins. *Biochemistry* 47, 6991–7000.
- Plowman SJ, Muncke C, Parton RG, Hancock JF (2005). H-ras, K-ras, and inner plasma membrane raft proteins operate in nanoclusters with differential dependence on the actin cytoskeleton. *Proc Natl Acad Sci USA* 102, 15500–15505.
- Raghupathy R, Anilkumar AA, Polley A, Singh PP, Yadav M, Johnson C, Suryawanshi S, Saikam V, Sawant SD, Panda A, et al. (2015). Transbilayer lipid interactions mediate nanoclustering of lipid-anchored proteins. *Cell* 161, 581–594.
- Regen SL (2020). The origin of lipid rafts. *Biochemistry* 59, 4617–4621.
- Ridone P, Pandzic E, Vassalli M, Cox CD, Macmillan A, Gottlieb PA, Martinac B (2020). Disruption of membrane cholesterol organization impairs the activity of PIEZO1 channel clusters. *J Gen Physiol* 152, e201912515.
- Rietveld A, Simons K (1998). The differential miscibility of lipids as the basis for the formation of functional membrane rafts. *Biochim Biophys Acta* 1376, 467–479.
- Ritchie K, Kusumi A (2002). Single molecule probe scanning optical force imaging microscope for viewing live cells. *J Biol Phys* 28, 619–626.
- Schneider F, Waithe D, Clausen MP, Galiani S, Koller T, Ozhan G, Eggeling C, Sezgin E (2017). Diffusion of lipids and GPI-anchored proteins in actin-free plasma membrane vesicles measured by STED-FCS. *Mol Biol Cell* 28, 1507–1518.
- Schubert C, Wedlich-Söldner R (2015). Building a patchwork—the yeast plasma membrane as model to study lateral domain formation. *Biochim Biophys Acta* 1853, 767–774.
- Sengupta P, Hammond A, Holowka D, Baird B (2008). Structural determinants for partitioning of lipids and proteins between coexisting fluid phases in giant plasma membrane vesicles. *Biochim Biophys Acta* 1778, 20–32.
- Seno K, Hayashi F (2017). Palmitoylation is a prerequisite for dimerization-dependent raftophilicity of rhodopsin. *J Biol Chem* 292, 15321–15328.
- Sevcsik E, Schütz GJ (2016). With or without rafts? Alternative views on cell membranes. *Bioessays* 38, 129–139.
- Seveau S, Bierne H, Giroux S, Prévost M-C, Cossart P (2004). Role of lipid rafts in E-cadherin- and HGF-R/Met-mediated entry of *Listeria monocytogenes* into host cells. *J Cell Biol* 166, 743–753.
- Sezgin E, Levental I, Grzybek M, Schwarzmann G, Mueller V, Honigsmann A, Below VN, Eggeling C, Coskun Ü, Simons K, et al. (2012a). Partitioning, diffusion, and ligand binding of raft lipid analogs in model and cellular plasma membranes. *Biochim Biophys Acta* 1818, 1777–1784.

- Sezgin E, Kaiser H-J, Baumgart T, Schwille P, Simons K, Levental I (2012b). Elucidating membrane structure and protein behavior using giant plasma membrane vesicles. *Nat Protoc* 7, 1042–1051.
- Sezgin E, Levental I, Mayor S, Eggeling C (2017). The mystery of membrane organization: composition, regulation and roles of lipid rafts. *Nat Rev Mol Cell Biol* 18, 361–374.
- Sezgin E, Schneider F, Galiani S, Urban I, Waithe D, Lagerholm BC, Eggeling C (2019). Measuring nanoscale diffusion dynamics in cellular membranes with super-resolution STED-FCS. *Nat Protoc* 14, 1054–1083.
- Sharma P, Varma R, Sarasij RC, Ira GK, Krishnamoorthy G, Rao M, Mayor S (2004). Nanoscale organization of multiple GPI-anchored proteins in living cell membranes. *Cell* 116, 577–589.
- Sheets ED, Holowka D, Baird B (1999). Critical role for cholesterol in Lyn-mediated tyrosine phosphorylation of FcεRI and their association with detergent-resistant membranes. *J Cell Biol* 145, 877–887.
- Shelby SA, Veatch SL, Holowka DA, Baird BA (2016). Functional nanoscale coupling of Lyn kinase with IgE-FcεRI is restricted by the actin cytoskeleton in early antigen-stimulated signaling. *Mol Biol Cell* 27, 3645–3658.
- Shimada Y, Maruya M, Iwashita S, Ohno-Iwashita Y (2002). The C-terminal domain of perfringolysin O is an essential cholesterol-binding unit targeting to cholesterol-rich microdomains. *Eur J Biochem* 269, 6195–6203.
- Shirai YM, Tsunoyama TA, Hiramoto-Yamaki N, Hirosawa KM, Shibata ACE, Kondo K, Tsurumune A, Ishidate F, Kusumi A, Fujiwara TK (2017). Cortical actin nodes: their dynamics and recruitment of podosomal proteins as revealed by super-resolution and single-molecule microscopy. *PLoS One* 12, e0188778.
- Simoncelli S, Griffié J, Williamson DJ, Bibby J, Bray C, Zamojska R, Cope AP, Owen DM (2020). Multi-color molecular visualization of signaling proteins reveals how C-terminal Src kinase nanoclusters regulate T cell receptor activation. *Cell Rep* 33, 108523.
- Simons K (2016). Cell membranes: a subjective perspective. *Biochim Biophys Acta* 1858, 2569–2572.
- Simons K, Ikonen E (1997). Functional rafts in cell membranes. *Nature* 387, 569–572.
- Simons K, Sampaio JL (2011). Membrane organization and lipid rafts. *Cold Spring Harb Perspect Biol* 3, a004697.
- Simons K, Toomre D (2000). Lipid rafts and signal transduction. *Nat Rev Mol Cell Biol* 1, 31–39.
- Simons K, van Meer G (1988). Lipid sorting in epithelial cells. *Biochemistry* 27, 6197–6202.
- Singer SJ, Nicolson GL (1972). The fluid mosaic model of the structure of cell membranes. *Science* 175, 720–731.
- Skočaj M, Resnik N, Grundner M, Ota K, Rojko N, Hodnik V, Anderluh G, Sobota A, Maček P, Veranič P, et al. (2014). Tracking cholesterol/sphingomyelin-rich membrane domains with the ostreolysin A-mCherry protein. *PLoS One* 9, e92783.
- Sohn HW, Tolar P, Pierce SK (2008). Membrane heterogeneities in the formation of B cell receptor–Lyn kinase microclusters and the immune synapse. *J Cell Biol* 182, 367–379.
- Štefanová I, Hořejší V, Ansoategui IJ, Knapp W, Stockinger H (1991). GPI-anchored cell-surface molecules complexed to protein tyrosine kinases. *Science* 254, 1016–1019.
- Stone MB, Shelby SA, Núñez MF, Wisser K, Veatch SL (2017). Protein sorting by lipid phase-like domains supports emergent signaling function in B lymphocyte plasma membranes. *eLife* 6, e19891.
- Stone MB, Veatch SL (2014). Steady-state cross-correlations for live two-colour super-resolution localization data sets. *Nat Commun* 6, 7347.
- Stulnig TM, Berger M, Sigmund T, Stockinger H, Hořejší V, Waldhäusl W (1997). Signal transduction via glycosyl phosphatidylinositol-anchored proteins in T cells is inhibited by lowering cellular cholesterol. *J Biol Chem* 272, 19242–19247.
- Subczynski WK, Antholine WE, Hyde JS, Kusumi A (1990). Microimmiscibility and three-dimensional dynamic structures of phosphatidylcholine-cholesterol membranes: translational diffusion of a copper complex in the membrane. *Biochemistry* 29, 7936–7945.
- Subczynski WK, Hyde JS, Kusumi A (1991). Effect of alkyl chain unsaturation and cholesterol intercalation on oxygen transport in membranes: a pulse ESR spin labeling study. *Biochemistry* 30, 8578–8590.
- Surviladze Z, Dráberová L, Kovářová M, Boubelík M, Dráber P (2001). Differential sensitivity to acute cholesterol lowering of activation mediated via the high-affinity IgE receptor and Thy-1 glycoprotein. *Eur J Immunol* 31, 1–10.
- Suzuki KGN, Fujiwara TK, Eddin M, Kusumi A (2007a). Dynamic recruitment of phospholipase C γ at transiently immobilized GPI-anchored receptor clusters induces IP $_3$ –Ca $^{2+}$ signaling: single-molecule tracking study 2. *J Cell Biol* 177, 731–742.
- Suzuki KGN, Fujiwara TK, Sanematsu F, Iino R, Eddin M, Kusumi A (2007b). GPI-anchored receptor clusters transiently recruit Lyn and G α for temporary cluster immobilization and Lyn activation: single-molecule tracking study 1. *J Cell Biol* 177, 717–730.
- Suzuki KGN, Kasai RS, Hirosawa KM, Nemoto YL, Ishibashi M, Miwa Y, Fujiwara TK, Kusumi A (2012). Transient GPI-anchored protein homodimers are units for raft organization and function. *Nat Chem Biol* 8, 774–783.
- Tanaka KAK, Suzuki KGN, Shirai YM, Shibutani ST, Miyahara MSH, Tsuboi H, Yahara M, Yoshimura A, Mayor S, Fujiwara TK, et al. (2010). Membrane molecules mobile even after chemical fixation. *Nat Methods* 7, 865–866.
- Tang B, Sun E-Z, Zhang Z-L, Liu S-L, Liu J, Kusumi A, Hu Z-H, Zeng T, Kang Y-F, Tang H-W, et al. (2022). Sphingomyelin-sequestered cholesterol domain recruits formin-binding protein 17 for constricting clathrin-coated pits in influenza virus entry. *J Virol* 96, e01813–21.
- Tiwari SS, Shirai YM, Nemoto YL, Kojima K, Suzuki KGN (2018). Native prion protein homodimers are destabilized by oligomeric amyloid β 1–42 species as shown by single-molecule imaging. *Neuroreport* 29, 106–111.
- Tomishige M, Sako Y, Kusumi A (1998). Regulation mechanism of the lateral diffusion of band 3 in erythrocyte membranes by the membrane skeleton. *J Cell Biol* 142, 989–1000.
- Tomishige N, Murate M, Didier P, Richert L, Mély Y, Kobayashi T (2021). The use of pore-forming toxins to image lipids and lipid domains. *Methods Enzymol* 649, 503–542.
- Trimble WS, Grinstein S (2015). Barriers to the free diffusion of proteins and lipids in the plasma membrane. *J Cell Biol* 208, 259–271.
- Tsuji A, Kawasaki K, Ohnishi S, Merkle H, Kusumi A (1988). Regulation of band 3 mobilities in erythrocyte ghost membranes by protein association and cytoskeletal meshwork. *Biochemistry* 27, 7447–7452.
- van Meer G, Voelker DR, Feigenson GW (2008). Membrane lipids: where they are and how they behave. *Nat Rev Mol Cell Biol* 9, 112–124.
- van Zanten TS, Cambi A, Koopman M, Joosten B, Figdor CG, Garcia-Parajo MF (2009). Hotspots of GPI-anchored proteins and integrin nanoclusters function as nucleation sites for cell adhesion. *Proc Natl Acad Sci USA* 106, 18557–18562.
- van Zanten TS, Gómez J, Manzo C, Cambi A, Buceta J, Reigada R, Garcia-Parajo MF (2010). Direct mapping of nanoscale compositional connectivity on intact cell membranes. *Proc Natl Acad Sci USA* 107, 15437–15442.
- Varma R, Mayor S (1998). GPI-anchored proteins are organized in submicron domains at the cell surface. *Nature* 394, 798–801.
- Veatch SL, Keller SL (2003). A closer look at the canonical “raft mixture” in model membrane studies. *Biophys J* 84, 725–726.
- Veerapathiran S, Wohland T (2018). The imaging FCS diffusion law in the presence of multiple diffusive modes. *Methods* 140, 140–150.
- Vial C, Evans RJ (2005). Disruption of lipid rafts inhibits P2X1 receptor-mediated currents and arterial vasoconstriction. *J Biol Chem* 280, 30705–30711.
- Wang X-D, Kim C, Zhang Y, Rindhe S, Cobb MH, Yu Y (2021). Cholesterol regulates the tumor adaptive resistance to MAPK pathway inhibition. *J Proteome Res* 12, 5379–5391.
- Wawrezynieck L, Rigneault H, Marguet D, Lenne P-F (2005). Fluorescence correlation spectroscopy diffusion laws to probe the submicron cell membrane organization. *Biophys J* 89, 4029–4042.
- Xia S, Lim YB, Zhang Z, Wang Y, Zhang S, Lim CT, Yim EK, Kanchanawong P (2019). Nanoscale architecture of the cortical actin cytoskeleton in embryonic stem cells. *Cell Rep* 28, 1251–1267.e7.
- Yamaji A, Sekizawa Y, Emoto K, Sakuraba H, Inoue K, Kobayashi H, Umeda M (1998). Lysenin, a novel sphingomyelin-specific binding protein. *J Biol Chem* 273, 5300–5306.
- Yu S, Sui Y, Wang J, Li Y, Li H, Cao Y, Chen L, Jiang L, Yuan C, Huang M (2022). Crystal structure and cellular functions of uPAR dimer. *Nat Commun* 13, 1665.
- Zhang Y, Bulkley DP, Xin Y, Roberts KJ, Asarnow DE, Sharma A, Myers BR, Cho W, Cheng Y, Beachy PA (2018). Structural basis for cholesterol transport-like activity of the hedgehog receptor patched. *Cell* 175, 1352–1364.e14.
- Zhou QD, Chi X, Lee MS, Hsieh WY, Mkrtchyan JJ, Feng A-C, He C, York AG, Bui VL, Kronenberger EB, et al. (2020). Interferon-mediated reprogramming of membrane cholesterol to evade bacterial toxins. *Nat Immunol* 21, 746–755.
- Zurzolo C, Simons K (2016). Glycosylphosphatidylinositol-anchored proteins: membrane organization and transport. *Biochim Biophys Acta* 1858, 632–639.